Acta Biochimica Polonica

Vol. 46 No. 3/1999

531–565

QUARTERLY

Review

Protein inhibitors of serine proteinases*°

Jacek Otlewski, Daniel Krowarsch and Wlodek Apostoluk

Institute of Biochemistry and Molecular Biology, University of Wrocław, Wrocław, Poland

Received: 21 June, 1999

Key words: serine proteinase, protein inhibitor, canonical conformation, protein–protein recognition

Serine proteinases and their natural protein inhibitors belong to the most intensively studied models of protein–protein recognition. Protein inhibitors do not form a single group but can be divided into about 20 different families. Global structures of proteins representing different inhibitor families are completely different and comprise α-helical proteins, β-sheet proteins, α/β-proteins and different folds of small disulfide-rich proteins. Three different types of inhibitors can be distinguished: canonical (standard mechanism) inhibitors, non-canonical inhibitors, and serpins. The canonical inhibitor binds to the enzyme through the exposed and convex binding loop, which is complementary to the active site of the enzyme. The mechanism of inhibition in this group is consistently very similar and resembles that of an ideal substrate. Non-canonical inhibitors, originating from blood sucking organisms, specifically block enzymes of the blood clotting cascade. The interaction is mediated through inhibitor N-terminus which binds to the proteinase forming a parallel β-sheet. There are also extensive secondary interactions which provide an additional buried area and contribute significantly to the strength and specificity of recognition. Serpins are major proteinase inhibitors occurring in plasma. Similarly to canonical inhibitors, serpins interact with their target proteinases in a substrate-like manner. However, in the case of serpins, cleavage of a single peptide bond in a flexible and exposed binding loop leads to dramatic structural changes.

---

*Presented at the symposium "Conformation of peptides, proteins and nucleic acids" held in Rynia, Poland, on 26–29 May, 1999.

°This work was supported by grant 6 P04B 002 10 from the State Committee for Scientific Research.

✉Author to whom correspondence should be addressed: Jacek Otlewski, Institute of Biochemistry and Molecular Biology, University of Wrocław, Tamka 2, 50-137 Wrocław, Poland; Phone: (48 71) 402 824; Fax: (48 71) 402 608; e-mail: otlewski@bf.uni.wroc.pl

Abbreviations: BPTI, bovine pancreatic trypsin inhibitor; TFPI, tissue factor pathway inhibitor; other inhibitors and proteinase abbreviations are listed in Tables 1 and 2.

Proteinases are hydrolytic enzymes which *in vivo* catalyse cleavage of peptide bonds in protein and peptide substrates. Proteolytic enzymes make use of an extremely broad range of substrate specificities applying several distinctly different chemical mechanisms to carry out peptide bond hydrolysis. There is a continuously growing recognition of the function of proteinases in a broad range of physiological processes of vital importance (Neurath, 1984; Czapinska & Otlewski, 1999). Proteinases are significant for extracellular metabolism playing a crucial role in defence mechanisms that protect an organism from tissue damage and infection (proteolytic cascades of blood coagulation, fibrinolysis and complement systems). Proteinases commonly act as regulatory elements through proteolytic activation of prohormones and zymogens, release of physiologically active peptides and are also active in macromolecular assembly of viruses and fibrin.

However, besides being necessary from the physiological point of view, proteinases are potentially hazardous to their proteinaceous environment and their activity must be precisely controlled by the respective cell or organism. When uncontrolled, proteinases can be responsible for serious diseases. The control of proteinases is normally achieved by regulated expression/secretion and/or activation of proproteinases, by degradation of mature enzymes, and by inhibition of their proteolytic activity. All known naturally occurring inhibitors directed towards endogenous cognate proteinases are proteins, only some microorganisms secrete small non-proteinaceous compounds which block the host proteinase activity. A huge number of inhibitors has been described, they were isolated from various cells, tissues and organisms. Often they accumulate in high quantities in plant seeds, bird eggs and various body fluids. Inhibitors of different types occur commonly among living organisms and viruses, what stresses their essential role in physiological processes.

Inhibition of proteinases by proteins itself appears to be a paradox. In fact, nature developed many different structural adaptations in protein structures to overcome the potential risk of proteolysis and develop specificity of recognition. Characterization of these conformational features is a principial goal of this review. Proteinase inhibitors adopt many different structures, ranging in size from mini-proteins to large macromolecular structures, much larger than the target enzyme.

From the structural point of view blocking of the enzyme active site is almost always achieved by docking of exposed structural elements, like loops or protein termini, either independently or in combination of two or more such elements. Canonical inhibitors of serine proteinases typically bind to target enzymes through a similarly shaped proteinase binding loop. Docking adjacent to the active site has been observed several times usually with simultaneous binding of an other part of inhibitor to the active site region. In one case the binding surfaces can be so distant from the active site of the enzyme that inhibition is effective only towards huge substrates having an extended interaction surface (Fuentes-Prior *et al.*, 1997). Interestingly, antibodies, despite enormous structural variability of their antigen binding loops, can not recognize the active site of antigenic enzymes, as they bind to flat or convex protein surfaces (Jones & Thornton, 1996).

Besides recognition of different surfaces in the active site area, some inhibitors directly utilize the mechanism of proteinase action to achieve inhibition. Up to the late 80s, the majority of the known proteinase inhibitors were substrate-like-binding molecules directed towards serine proteinases blocking the enzyme at the distorted Michaelis complex reaction stage (Bode & Huber, 1992). In the case of these canonical inhibitors, permanent inhibi-

tion results from a rather peculiar thermodynamic property of a single peptide bond, the value for its hydrolysis being extremely low (Laskowski & Kato, 1980). The recently described bacterial inhibitor of metalloproteinases appears to resemble canonical inhibitors in this respect (Seeram *et al.*, 1997). Conversely, another group of serine proteinase inhibitors – serpins – exhibits an extremely high, virtually irreversible, value of the reactive site hydrolysis and utilizes kinetic features of the hydrolytic reaction to form a complex at the (metastable) acyl enzyme intermediate (Stone *et al.*, 1997).

INHIBITORS OF SERINE PROTEINASES

Serine proteinases and their protein inhibitors have been the most intensively studied group of protein–protein complexes. Currently, a large number of three-dimensional structures is available for representatives of 15 inhibitor families (Table 1). For some inhibitors, particularly members of BPTI, Kazal, potato I families many structures have been determined both for different free inhibitors and for their enzyme complexes.

Protein inhibitors of serine enzymes do not use a single mechanism to inhibit the cognate proteinase. Instead, three different inhibition mechanisms can be currently distinguished. The largest group is formed by canonical inhibitors which act according to the standard mechanism (Laskowski & Kato, 1980). Canonical inhibitors are widely distributed in essentially all groups of organisms and comprise proteins from 27 to about 200 amino-acid residues. The standard mechanism implies that inhibitors are peculiar protein substrates containing the reactive site P_1-P_1' peptide bond located in the most exposed region of the proteinase binding loop (P_1, P_2 and P_1', P_2' designate inhibitor residues amino- and carboxy-terminal to the scissile peptide bond; S_1, S_2 and S_1', S_2' denote the corresponding subsites on the proteinase (Schechter & Berger, 1967)). The reactive site can be selectively hydrolyzed by the enzyme. The binding loop is in similar, so called canonical, conformation in inhibitor structures representing different families (Bode & Huber, 1992; Apostoluk & Otlewski, 1998). It is usually assumed and in most cases has been verified experimentally that the standard mechanism inhibitors show canonical conformation of the binding loop.

Non-canonical inhibitors bind to the enzyme active site through their N-terminal segment but also contact the proteinase at more distant site(s). Due to the extensive contact area, these inhibitors form very tight and specific complexes with serine proteinases. The classic example is recognition of thrombin by hirudin (Stubbs & Bode, 1995). Interestingly, such an interaction features also proteins possessing folds of canonical inhibitors like BPTI- or Kazal-type inhibitors but with distorted conformation of the binding loop.

Serpins (*ser*ine *p*roteinase *in*hibitors) are single domain proteins of about 400 amino-acid residues which are abundant in plasma often in variably glycosylated forms (Travis & Salvesen, 1983; Potempa *et al.*, 1994). Like the canonical inhibitors, they interact with their target enzyme in a substrate-like manner through the exposed loop of poorly defined structure. In the case of serpins, however, cleavage of the P_1-P_1' peptide bond leads to dramatic structural and stability changes (Whisstock *et al.*, 1998). In contrast to canonical inhibitors, the reactive site loop of serpins is flexible and can assume a number of different conformations. Serpins are the only family of serine proteinase inhibitors for which complex formation with non-serine enzymes – cysteine proteinases (Komiyama *et al.*, 1994) and aspartyl proteinases (Mathialagan & Hansen, 1996) has been demonstrated.

Table 1. Three-dimensional structures of protein inhibitors of serine proteinases and their enzyme complexes.

The structures were determined by X-ray or NMR methods. Generally, in the case of crystallographically determined structures, only structures with the highest resolution are indicated. The table contains all inhibitor and proteinase abbreviations used in this paper.

Family	Structure	Abbreviation	PDB code	Method	Reference
Ecotin	Ecotin	Ecotin	1ECY	X-ray (2.2 Å)	Shin *et al.*, 1996
	Ecotin:rat anionic trypsin	Ecotin:rTP		X-ray (2.4 Å)	McGrath *et al.*, 1994
	Ecotin:crab collagenase	Ecotin:cCOLL	1AZZ	X-ray (2.3 Å)	Perona *et al.*, 1997
Ascaris inhibitor	*Ascaris* trypsin inhibitor (pH 4.75)	ATI (pH 4.75)	1ATA	NMR	Grasberger *et al.*, 1994
	ATI (pH 2.4)	ATI (pH 2.4)	1ATB	NMR	Grasberger *et al.*, 1994
	Ascaris chymotrypsin/elastase inhibitor:porcine pancreatic elastase	C/E-1:PPE		X-ray (2.4 Å)	Huang *et al.*, 1994
Hirustasin	Antistasin	Antistasin	1SKZ	X-ray (1.9 Å)	Lapatto *et al.*, 1997
	Hirustasin	Hirustasin	1BX7	X-ray (1.2 Å)	Uson *et al.*, 1999
	Hirustasin:porcine kallikrein	Hirustasin: pKALL	1HIA	X-ray (2.4 Å)	Mittl *et al.*, 1996
Cereal inhibitor	Ragi bifunctional α-amylase/trypsin inhibitor	RBI	1BLU	X-ray (2.9 Å)	Gourinath *et al.*, 1999
	RBI	RBI	1BIP	NMR	Strobl *et al.*, 1995
	RBI:yellow meal worm α-amylase	RBI:TMA	1TMQ	X-ray (2.5 Å)	Strobl *et al.*, 1998
	Corn Hageman factor inhibitor	CHFI	1BEA	X-ray (1.9 Å)	Behnke *et al.*, 1998
	Barley α-amylase/subtilisin inhibitor:barley α-amylase	BASI:AMY2	1AVA	X-ray (1.9 Å)	Vallée *et al.*, 1998
STI	Soybean trypsin inhibitor	STI	1AVU	X-ray (2.3 Å)	Song & Suh, 1998
	STI:pTP (orthorombic)	STI:pTP	1AVW	X-ray (1.7 Å)	Song & Suh, 1998
	Erythrina caffra trypsin inhibitor	ETI	1TIE	X-ray (2.5 Å)	Onesti *et al.*, 1991
	Bifunctional proteinase K/α-amylase inhibitor	PKI3		X-ray (2.5 Å)	Zemke *et al.*, 1991
	PKI3:proteinase K	PKI3:PK		X-ray (2.5 Å)	Pal *et al.*, 1994
	Winged bean chymotrypsin inhibitor	WCI	2WBC	X-ray (2.3 Å)	Dattagupta *et al.*, 1999
BPTI	BPTI (crystal form II)	BPTI (II)	5PTI	X-ray/neutron (0.98 Å)	Wlodawer *et al.*, 1984
	BPTI	BPTI	1PIT	NMR	Berndt *et al.*, 1992
	BPTI:bovine trypsin	BPTI:bTP	2PTC	X-ray (1.9 Å)	Huber *et al.*, 1974
	BPTI:bovine anhydrotrypsin	BPTI:bTPan	1TPA	X-ray (1.9 Å)	Huber *et al.*, 1975
	BPTI:rTP mutant	BPTI:rTP (D189G,G226D)	1BRB	X-ray (2.1 Å)	Perona *et al.*, 1993
	BPTI:anionic salmon trypsin	BPTI:sTP	1BZX	X-ray (2.1 Å)	Helland *et al.*, 1998
	BPTI:bovine chymotrypsin	BPTI:bCHTP	1CBW	X-ray (2.6 Å)	Scheidig *et al.*, 1997

	BPTI:porcine kallikrein A	BPTI:pKALL	2KAI	X-ray (2.5 Å)	Chen & Bode, 1983
	BPTI:human thrombin mutant	BPTI:hTHRO (E192Q)	1BTH	X-ray (2.3 Å)	van de Locht *et al.*, 1997
	BPTI mutant:factor VIIa: tissue factor	BPTI (5L15): factor VIIa:TF		X-ray (2.1 Å)	Zhang *et al.*, 1999
	BPTI:bovine trypsinogen	BPTI:bTPG	2TGP	X-ray (1.9 Å)	Bode *et al.*, 1978
	BPTI:bTPG:Ile-Val	BPTI:bTPG:IV	3TPI	X-ray (1.9 Å)	Bode *et al.*, 1978
	Amyloid β-protein precursor inhibitor domain:rTP	APPI:rTP	1AAP	X-ray (1.5 Å)	Hynes *et al.*, 1990
	APPI	APPI		NMR	Heald *et al.*, 1991
	APPI:rTP mutant	APPI:rTP (D189G,G226D)	1BRC	X-ray (2.5 Å)	Perona *et al.*, 1993
	APPI:bTP	APPI:bTP	1TAW	X-ray (1.8 Å)	Scheidig *et al.*, 1997
	APPI:bCHTP	APPI:bCHTP	1CA0	X-ray (2.1 Å)	Scheidig *et al.*, 1997
	Second domain of human tissue factor pathway inhibitor	hTPPI	1ADZ	NMR	Burgering *et al.*, 1997
	hTPPI:porcine trypsin	hTPPI:pTP	1TFX	X-ray (2.6 Å)	Burgering *et al.*, 1997
	Bikunin	Bikunin	1BIK	X-ray (2.5 Å)	Xu *et al.*, 1998
	Proteinase inhibitor from sea anemone	ShPI	1SHP	NMR	Antuch *et al.*, 1993
	α3 Chain of human type VI collagen	Domain C5	2KNT	X-ray (1.2 Å)	Merigeau *et al.*, 1998
	Domain C5	Domain C5	1KUN	NMR	Zweckstetter *et al.*, 1995
Kazal	Silver pheasant ovomucoid third domain	OMSVP3	2OVO	X-ray (1.5 Å)	Bode *et al.*, 1985
	OMSVP3 (reactive site hydrolyzed)	OMSVP3*	4OVO	X-ray (2.5 Å)	Musil *et al.* 1991
	Turkey ovomucoid third domain	OMTKY3		NMR	Krezel *et al.*, 1994
	OMTKY3 (reactive site hydrolyzed)	OMTKY3*	1TUS	NMR	Walkenhorst *et al.*, 1994
	OMTKY3: human neutrophil elastase	OMTKY3: hNE	1PPF	X-ray (1.7 Å)	Bode *et al.*, 1986a
	OMTKY3:bovine α-chymotrypsin	OMTKY3: bCHYM	1CHO	X-ray (1.8 Å)	Fujinaga *et al.*, 1987
	OMTKY3:*Streptomyces griseus* proteinase B	OMTKY3: SGPB	3SGB	X-ray (1.8 Å)	Fujinaga *et al.*, 1982; Read *et al.*, 1983
	Human pancreatic secretory trypsin inhibitor mutant	hPSTI (K18Y, I19E, D21R, N29D)	1HPT	X-ray (2.3 Å)	Hecht *et al.*, 1992
	Porcine PSTI: bovine trypsinogen	pPSTI:pTG	1TGS	X-ray (1.8 Å)	Bolognesi *et al.*, 1982
	Human PSTI: bovine chymotrypsinogen A	hPSTI: pCHTG			Hecht *et al.*, 1991
	Rhodniin:bovine thrombin	rhodniin: bTHRO	1TBQ	X-ray (2.6 Å)	van de Locht *et al.*, 1995
	Leech-derived tryptase inhibitor	LDTI-C		NMR	Mühlhahn *et al.*, 1994

	LDTI-C:porcine trypsin	LDTI:pTP	1LDT	X-ray (1.9 Å)	Priestle & Di Marco, 1997
	Porcine PEC-60	PEC-60	1PCE	NMR	Liepinsh *et al.*, 1994
Potato inhibitor 1	Barley proteinase inhibitor 2	CI-2	2CI2	X-ray (2.0 Å)	McPhalen & James, 1987
	CI-2	CI-2	3CI2	NMR	Ludvigsen *et al.*, 1991
	CI-2:subtilisin BPN'	CI-2:SBPN	2SNI	X-ray (2.1 Å)	McPhalen & James, 1988
	Eglin c	eglin		X-ray (1.9 Å)	Hipler *et al.*, 1992
	Eglin	eglin	1EGL	NMR	Hyberts *et al.*, 1992
	Eglin (reactive site hydrolyzed)	eglin*	1EGP	X-ray (2.0 Å)	Betzel *et al.*, 1993
	Eglin:SBPN	eglin:SBPN	1SIB	X-ray (2.4 Å)	Heinz *et al.*, 1991
	Eglin:subtilisin Carlsberg	eglin:SCARL	1CSE	X-ray (1.2 Å)	Bode *et al.*, 1986b
	Eglin:subtilisin mesentericus	eglin:SBMEP	1MEE	X-ray (2.0 Å)	Dauter *et al.*, 1991
	Eglin:thermitase	eglin:THER	1TEC	X-ray (2.2 Å)	Gros *et al.*, 1992
	Eglin:bCHYM	eglin:bCHYM	1ACB	X-ray (2.0 Å)	Bolognesi *et al.*, 1990
	Cucurbita maxima trypsin inhibitor-V	CMTI-V		NMR	Cai *et al.*, 1995a
	CMTI-V (reactive site hydrolyzed)	CMTI-V*	1HYM	NMR	Cai *et al.*, 1995b
Potato inhibitor 2	Polypeptide inhibitor:SGPB	PCI:SGPB	4SGB	X-ray (2.1 Å)	Greenblatt *et al.*, 1989
	Nicotiana alata proteinase inhibitor C1	Na-C1		NMR	Nielsen *et al.*, 1994b
	Nicotiana alata proteinase inhibitor isoforms	Na-T1, Na-T2, Na-T3, Na-T4	1TIH	NMR	Nielsen *et al.*, 1995
SSI	*Streptomyces* subtilisin inhibitor	SSI	3SSI	X-ray (2.3 Å)	Mitsui *et al.*, 1977
	SSI:SBPN	SSI:SBPN	2SIC	X-ray (1.8 Å)	Takeuchi *et al.*, 1991
	SSI mutant:bTP	SSI (M70G, M73K):bTP	2TLD	X-ray (2.6 Å)	Takeuchi *et al.*, 1992
Chelonianin	Mucous proteinase inhibitor:bCHYM	MPI:bCHYM		X-ray (2.5 Å)	Grütter *et al.*, 1988
	Elafin	Elafin	1REL	NMR	Francart *et al.*, 1997
	Elafin:porcine pancreatic elastase	elafin:PPE	1FLE	X-ray (1.9 Å)	Tsunemi *et al.*, 1996
Bowman-Birk inhibitor	Soybean trypsin/chymotrypsin Bowman-Birk inhibitor	BBI-I	1BBI 2BBI	NMR	Werner & Wemmer, 1992
	Peanut protease inhibitor A-II	A-II		X-ray (2.3 Å)	Suzuki *et al.*, 1993
	Soybean proteinase inhibitor II	PI-II	1PI2	X-ray (2.5 Å)	Chen *et al.*, 1992
	Winter pea trypsin/ chymotrypsin inhibitor	PsTI	1PBI	X-ray (2.7 Å)	Li de la Sierra *et al.*, 1999
	Azuki bean protease inhibitor:bTP	AB-I:bTP	1TAB	X-ray (3.0 Å)	Tsunogae *et al.*, 1986
	Mung bean trypsin inhibitor:pTP	MBTI:pTP		X-ray (2.5 Å)	Lin *et al.*, 1993
Sqash seed inhibitor	*Cucurbita maxima* trypsin inhibitor I	CMTI I	1CTI 3CTI	NMR	Holak *et al.*, 1989; 1991

	CMTI I:bTP	CMTI I:bTP	1PPE	X-ray (2.0 Å)	Bode *et al.*, 1989
	CMTI I:sTP	CMTI I:sTP		X-ray (1.8 Å)	Helland *et al.*, 1999b
	Cucurbita pepo trypsin inhibitor II:bTP	CPTI II:bTP		X-ray (1.5 Å)	Helland *et al.*, 1999b
	CPTI II:sTP	CPTI II:sTP		X-ray (1.8 Å)	Helland *et al.*, 1999b
	MCTI-A:pTP	MCTI-A:pTP		X-ray (1.6 Å)	Huang *et al.*, 1992
	Ecbalium elaterium trypsin inhibitor II	EETI II	2ETI	NMR	Heitz *et al.*, 1989; Chiche *et al.*, 1989
	Trypsin carboxypeptidase peptide inhibitor	TCPI		NMR	Chiche *et al.*, 1993
Locusta hemolymph inhibitor	*Locusta migratoria* inhibitor D2	PMP-D2		NMR	Mer *et al.*, 1994
	Locusta migratoria inhibitor C	PMP-C	1PMC	NMR	Mer *et al.*, 1996
Non-canonical inhibitors	Ornithodorin:bTHRO	ornithodorin: bTHRO	1TOC	X-ray (3.1 Å)	van de Locht *et al.*, 1996
	Tick anticoagulant peptide	TAP	1TAP	NMR	Lim-Wilby *et al.*, 1995
	TAP:bovine factor Xa	TAP:bFXa	1KIG	X-ray (3.0 Å)	Wei *et al.*, 1998
	Triabin-bTHRO	Triabin-bTHRO	1AVG	X-ray (2.6 Å)	Fuentes-Prior *et al.*, 1997
	Desulfato hirudin	hirudin 1	5HIR	NMR	Folkers *et al.*, 1989
	Hirudin 1:hTHRO	hirudin 1:hTHRO		X-ray (2.9 Å)	Grütter *et al.*, 1990

THE CANONICAL OR STANDARD MECHANISM INHIBITORS

The inhibitor

Global structures of proteins belonging to different inhibitor families comprise different folds of α-helical, β-sheet, mixed α/β and small disulfide-rich proteins. Examples of different folds of inhibitor structures which were determined in recent years are shown in Figs. 1 to 7. All inhibitors feature similar, canonical conformation of the binding loop which is supported by a single domain of globular structure. In the case of several families (BPTI, Kazal, Bowman-Birk, chelonianin) the single domain structure is repeated 2, 3, 4 or 7 times to form a multidomain, single chain inhibitor which is able to independently interact with several proteinases at separate reactive sites. More surprisingly, there are currently known examples of inhibitors from two families (cereal family – RBI and BASI; STI family – PKI3) which can inhibit not only serine proteinase but also α-amylase at independent binding sites.

The convex proteinase binding loop exhibits an extended conformation which significantly protrudes from the protein scaffold and serves as a rather simple recognition motif (Fig. 8). The loop forms a sequential epitope spanning from position P_3 to P_3'. Residues that precede or follow this segment (e.g. P_6 or P_4') and residues from a sequentially remote region, called the secondary contact region, can also contact the enzyme and influence the association energy. The central section of the loop contains solvent exposed P_1-P_1' peptide bond, called the reactive site which can be cleaved by a serine proteinase. The equilibrium value of the reactive site peptide bond opening, called the hydrolysis constant, is

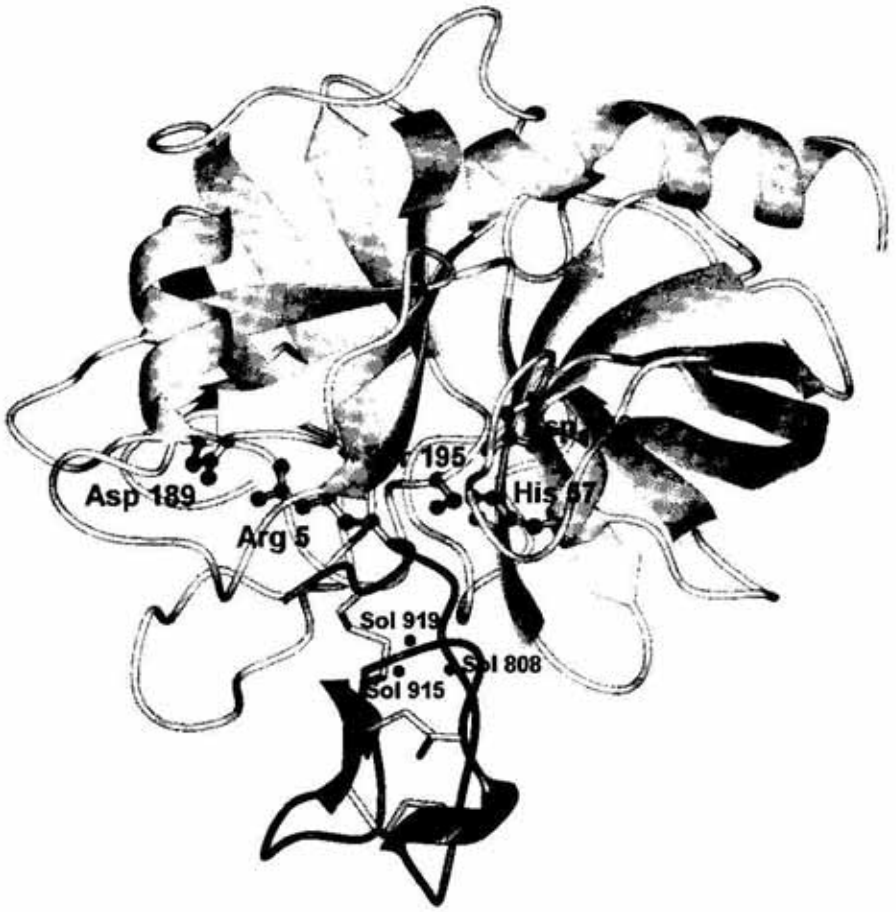

Figure 1. α-Carbon drawing of the complex formed between bovine β-trypsin (light grey) and CMTI I (dark grey) (Bode *et al.*, 1989).

The 29-residue inhibitor belongs to the smallest known protein inhibitors. The major interactions comprise the proteinase binding residues: Val2 (P4) to Glu9 (P4′). Important side chains of inhibitor which are shown: the Arg5 (P_1) side chain which is involved in almost half of the contacts with trypsin; Cys3-Cys20, Cys10-Cys22 and Cys16-Cys28 disulfide bonds (the major structural stability and rigidity determinants); internal water molecules Sol808, Sol915 and Sol919 (dark balls) which stabilize loop conformation through a system of hydrogen bonds to protein scaffold. On the enzyme side Asp189 and the catalytic triad (Ser195, His57, Asp102) are shown.

usually not far away from unity (Ardelt & Laskowski, 1991; Siekmann *et al.*, 1988; Otlewski & Zbyryt, 1994). The conformation of the cleaved inhibitor is very similar to that of its intact form with clear exceptions for local structural changes near the P_1-P_1' peptide bond (Musil *et al.*, 1991; Betzel *et al.*, 1993) and increased internal mobility of the cleaved loop, but not of the inhibitor scaffold (Shaw *et al.*, 1995; Liu *et al.*, 1996a). Thermodynamic analysis reveals that hydrolysis of the reactive site in native inhibitor does not lead to a significant increase in entropy; the full entropy gain is realized upon denaturation of the reactive site cleaved inhibitor, this leading to predicted values of K_{hyd} for the hydrolysis of the reactive site in denatured inhibitor on the level of 100 (Laskowski & Sealock, 1971; Krokoszynska & Otlewski, 1996).

Main chain conformations of the binding loops of free inhibitors representing different families are similar and become even more similar on the inhibitor–enzyme complex formation (Apostoluk & Otlewski, 1998). The canonical conformation is presumed to be adopted also by a productively bound protein substrate. Binding loops within one family, most intensively studied for Kazal inhibitors

Figure 2. Ribbon presentation of the tetrameric ecotin:crab collagenase complex (ecotin:cCOLL) (Perona *et al.*, 1997).

There are three major areas of interaction: one at the ecotin dimer interface and two at the primary (the reactive site, 80s loop and 50s loop) and the secondary (loops 60s and 100s) binding sites with trypsin. The trypsin molecules are light grey and ecotin monomers are dark grey.

(Laskowski *et al.*, 1987), often show high sequential variability, nevertheless, in all studied cases the loops preserve the canonical conformation. On the other hand, sequences of the binding loops also show many clear amino acid preferences. For example, half cystine is present either at P_3 (Kazal, squash, SSI, potato 2, *Ascaris* families) or at P_2 (BPTI, hirustasin, chelonianin families) positions; Thr is often met at P_2 (Kazal, potato 1, Bow-

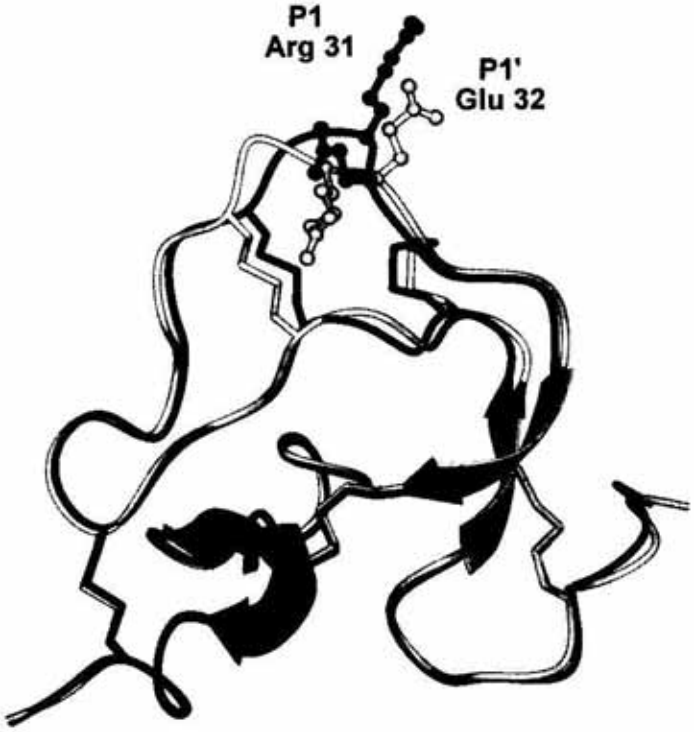

Figure 3. The backbone superpositions of the mean structures of *Ascaris* trypsin inhibitor at pH 2.4 (ATI pH 2.4, dark grey) and pH 4.75 (ATI pH 4.75, light grey) (Grasberger *et al.*, 1994).

The proteinase binding loop (containing the reactive site Arg31-Glu32 shown on the Figure) is spanned between Cys15-Cys33 and Cys18-Cys29 disulfide bonds, it is shown in two different pH-induced conformations. The low pH conformation is similar to the canonical conformation of other inhibitors. At pH 4.5 the loop's conformation is deformed, which possibly is of physiological meaning. Four short β-strands arranged in two perpendicular β-sheets and remaining three disulfide bonds: Cys5-Cys38, Cys22-Cys60 and Cys40-Cys54 are also indicated.

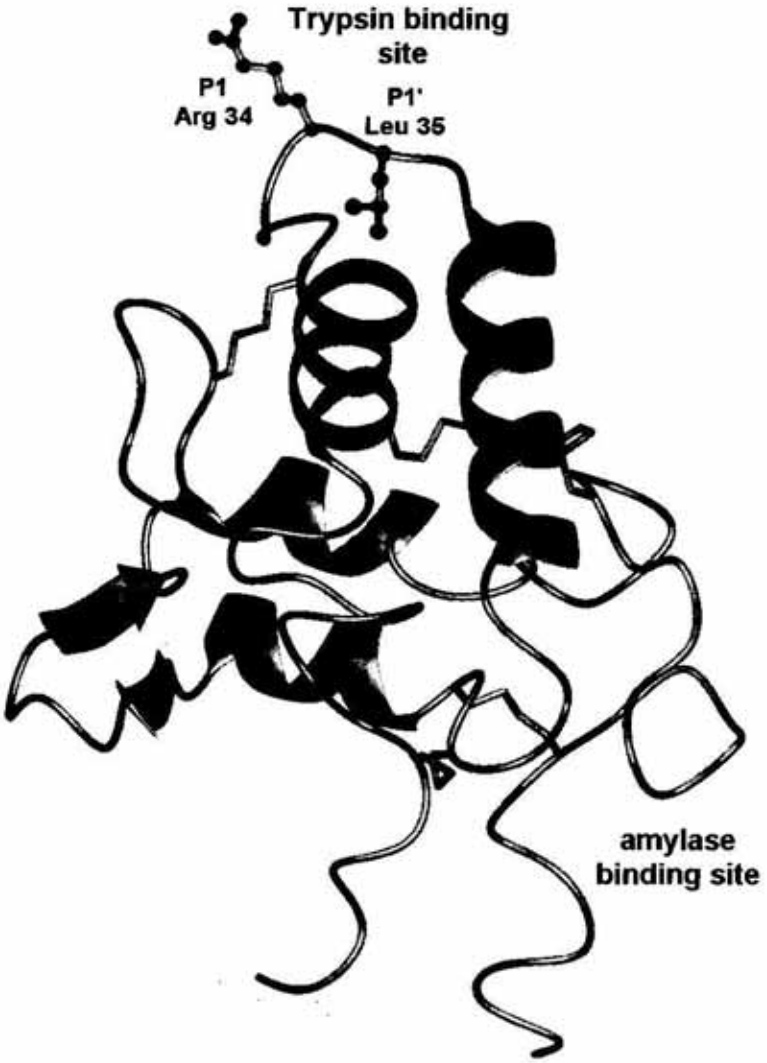

Figure 4. Ribbon drawing of the 122-residue protein ragi bifunctional trypsin/α-amylase inhibitor, as determined in solution by NMR spectroscopy (Strobl *et al.*, 1995).

The side chains of reactive site Arg34-Leu35 peptide bond are indicated together with secondary structure elements and five disulfide bridges. The canonical conformation of the loop is spanned between two adjacent helices, a structural feature unique to this inhibitor family. Inhibition of α-amylase occurs at completely independent and spatially remote segments 1 (Ser1-Ala11, Pro52-Cys55) and 2 (Val67-Ser70, Thr107-Gly110, Leu115-Leu117) of RBI (Strobl *et al.*,

man-Birk, SSI, ecotin, *Ascaris* families) and Pro is fully conserved at P_3 in STI family (Apostoluk & Otlewski, 1998). Ile is fully conserved at P_1˜ position in the squash family. Its mutation to Leu leads to severe disordering of the binding loop (Nielsen *et al.*, 1994a). Similar disordering of the loop was observed upon D46S (P_1˜) in eglin c (Heinz *et al.*, 1992). Thus, there are multiple sequential ways to achieve the canonical conformation.

The loop conformation results from a rather extensive system of hydrogen bonds and hydrophobic interactions which involve residues both from the loop and the inhibitor scaffolding. In OMSVP3 and CI-2 inhibitors carbonyl oxygens of P_2 and P_1' are involved in hydrogen bonds to side chains of Asn33 and Arg65, respectively. In BPTI and CMTI I similar interactions are mediated through water molecules to Gly12 and to the side chain of Cys20, respectively. Substitution of the residues which maintain loop conformation affects the value of K_{hyd}, the effect of a single mutation is, however, relatively small, not exceeding factor 3 to 5 (Ardelt & Laskowski, 1991). Moreover, there is evidence, based on changes in ^{15}N relaxation rates, for increased dynamics of the loop in CMTI-V mutants with eliminated side chains of Arg50 or Arg52 which anchor the loop conformation to the scaffold (Cai *et al.*, 1996). Mutation of these two side chains in homologous eglin c led to a decrease in inhibitory potential (Heinz *et al.*, 1992). Replacement of the CI-2 loop sequence with that of helix E from subtilisin Carlsberg leads to formation of a protein hybrid with a well preserved scaffold and extended loop-like conformation of the introduced sequence (Osmark *et*

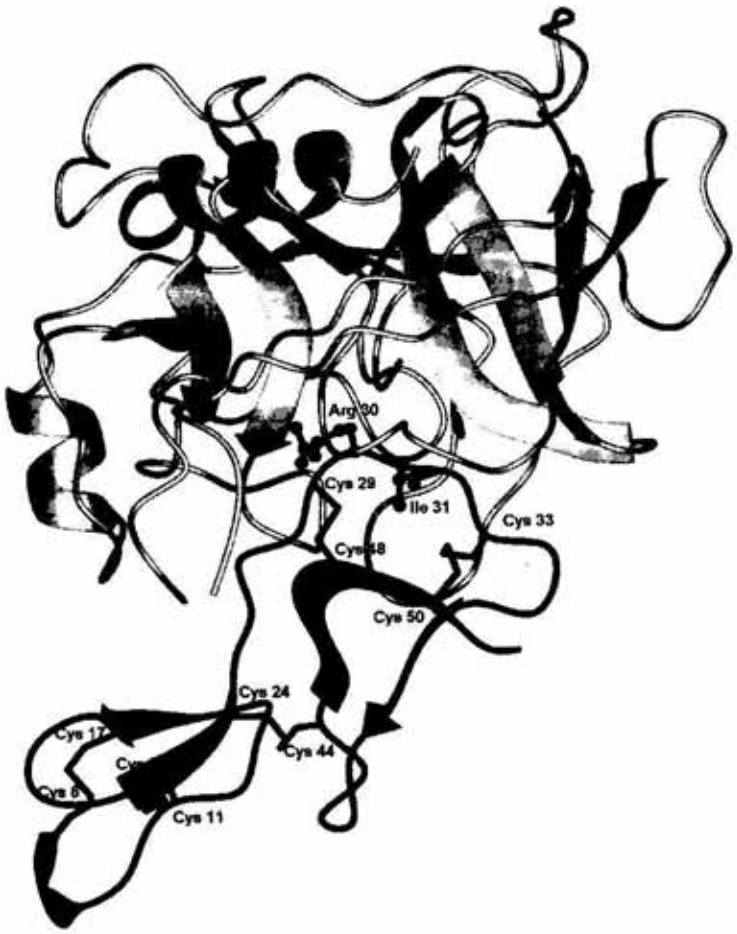

Figure 5. Ribbon diagram of the overall structure of hirustasin (dark grey) as seen in the complex with porcine tissue kallikrein (hirustasin:pKALL light grey) (Mittl *et al.*, 1996).

The five disulfides and the reactive site Arg30-Ile31, which serves to inhibit kallikrein, are indicated. There are four short β-strands indicated by arrows in this otherwise random coil structure. A homologous inhibitor of factor Xa – antistasin is composed of two hirustasin-like domains. Modelling studies show that the N-terminal domain is involved in factor Xa binding (Lapatto *et al.*, 1997).

al., 1993). This shows that the context of CI-2 scaffold is able to deform a helix to a loop conformation. The inhibitor scaffold, therefore, seems to play an active role in maintaining loop conformation. The loops of canonical conformation can be occasionally found in non-inhibitory proteins, it is unlikely, however, that they can inhibit serine proteinases due to insufficient protrusion of such loops from protein scaffolds (Apostoluk & Otlewski, 1998).

There are examples of proteins, like snake toxins, which show high sequence and tertiary structure similarities to inhibitors of BPTI family, including conformation of the proteinase binding loop, yet, they do not inhibit any tested serine proteinase. In one tested case of non-inhibitory C5 domain (BPTI family member) it was possible to generate a strong antiproteinase inhibitor through multiple substitutions in the binding loop region (Kohfeld *et al.*, 1996). However, in many other cases conversion of a non-inhibitory to inhibitory protein could require more effort due to severe conformational and dynamic changes in the binding loop region.

The inhibitor scaffolds are of very different structural types. In several inhibitor families, like BPTI, Kazal, potato 1 and 2, cereal, SSI, STI, and ecotin, elements of a typical secondary structure together with the presence of hydrophobic core can be distinguished. Other, including squash, Bowman-Birk, *Locusta* haemolymph, hirustasin, chelonianin, and *Ascaris* families essentially lack the hydrophobic core and extensive secondary structure elements. For these inhibitors disulfide bonds, which are usually buried inside the molecule, are major determinants of protein stability.

Inhibitors belonging to different families are stable proteins resistant to high denaturation temperatures and to chemical denaturants. In

Figure 6. Superposition of the main chain of non-classical Kazal inhibitor – leech-derived trypsin inhibitor (LDTI) (dark grey) (Stubbs *et al.*, 1997) and classical Kazal inhibitor silver pheasant ovomucoid third domain (OMSVP3) (light grey) (Bode *et al.*, 1985).

A highly unique feature of LDTI is the strong inhibition of tryptase. Due to a large deletion, the α-helix of LDTI is one turn shorter than in OMSVP3 and the N-terminus, again due to a large deletion, is closer to the α-helix. The smaller size of LDTI enables binding of two inhibitor molecules at two diagonally located active sites of the central pore of tryptase tetramer (Pereira *et al.*, 1998).

particular, BPTI shows a denaturation temperature of about 100°C and is stable in 6 M guanidinum chloride (Moses & Hinz, 1983; Makhatadze *et al.*, 1993). Inhibitors are often cross-linked with conserved disulfide bonds. The topology of disulfide bonds is preserved within a single family. However, some members of potato I family show either no S–S bond or a single disulfide. Selective reduction or elimination of disulfide bond(s) leads usually to a significant destabilization of an inhibitor molecule, to lower association energy, and to greater sensitivity to proteolysis (Hurle *et al.*, 1990; Yu *et al.*, 1995; Krokoszynska *et al.*, 1998). The same holds for destabilizing mutation(s) introduced into the inhibitor core (Tamura *et al.*, 1991; Beeser *et al.*, 1997). Thus, stability of the inhibitor scaffold seems to be essential for efficient inhibition.

The standard mechanism

The canonical inhibitor – cognate proteinase interaction, called the standard mechanism, resembles in several aspects hydrolysis of a single peptide bond in regular protein substrates (Laskowski & Kato, 1980). The interaction can be presented as a hydrolysis/resynthesis reaction of the reactive site P_1-P_1' peptide bond:

$$E + I \underset{k_{off}}{\overset{k_{on}}{\rightleftharpoons}} EI \underset{k_{on}^*}{\overset{k_{off}^*}{\rightleftharpoons}} E + I^* \qquad (1)$$

where E is the proteinase, I the inhibitor, I* the reactive site cleaved inhibitor, EI the stable complex, k_{on} and k_{on}^* are respective second order association rate constants, and k_{off} and k_{off}^* are respective first order dissociation rate constants of the complex.

However, compared to regular protein peptide bond hydrolysis:

(i) the complex EI is much more stable than Michaelis ES complex. Typical inhibition constant (K_i) values are 10^6–10^9-fold lower than K_m values. EI complex can be crystallized and shows all typical features of a protein–protein recognition (Janin & Chothia, 1990; Jones & Thornton, 1996),

(ii) the catalytic rate constant for hydrolysis of the reactive site is extremely slow at neutral pH (Finkenstadt *et al.*, 1974; Otlewski & Zbyryt, 1994). However, there are known examples of hydrolysis of reactive sites by in-

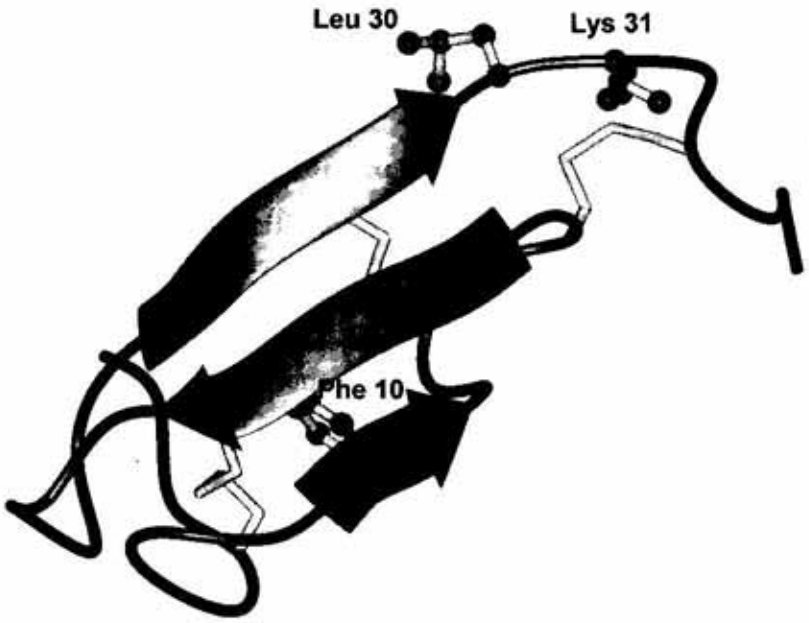

Figure 7. Ribbon presentation of the solution structure of a 36-residue proteinase inhibitor from *Locusta migratoria* (PMP-C) (Mer *et al.*, 1996).

The inhibitor conformation consists of three stranded antiparallel β-sheets forming a cavity filled with a Phe10 (shown). The reactive site peptide bond Leu30-Lys31 (shown) is located at the C-terminal segment side chain, and tensed between two disulfide bonds: Cys17-Cys28 and Cys14-Cys33 (the third disulfide is formed between Cys4 and Cys19). A unique feature of the protein is the ability to inhibit not only serine proteinases but also to block high voltage-activated Ca^{2+} currents in rat neurones (Harding *et al.*, 1995).

hibited proteinases which proceed at relatively high rates (Estell *et al.*, 1980, Ardelt & Laskowski, 1983).

(iii) many different serine proteinases (belonging both to chymotrypsin and subtilisin families) of completely different specificities are inhibited at the same reactive site (Ardelt & Laskowski, 1985). This results from the similar mode of recognition between the proteinase binding loop and the active site.

(iv) k_{cat}/K_m index for the hydrolysis of the reactive site peptide bond is high, suggesting that inhibitors are good substrates (Finkenstadt *et al.*, 1974). However, the index features the enzyme–substrate reaction only at very low ([S] < K_m) substrate concentrations. Since the K_m values for hydrolysis are extremely low, the reaction rate is proportional to k_{cat} which is known to be extremely low in the case of reactive site hydrolysis.

(v) the hydrolysis reaction is reversible, i.e. the cleaved inhibitor is active and forms the same complex with the enzyme as the intact form. During complex formation from cleaved inhibitor side the resynthesis of the reactive site peptide bond occurs (Finkenstadt & Laskowski, 1967). Kinetic parameters for the reactive site resynthesis are often similar to those of hydrolysis. The phenomenon of hydrolysis/resynthesis occurs also at other peptide bonds of the binding loop and can be also catalyzed by non-serine proteinases (Otlewski *et al.*, 1994).

(vi) the equilibrium value of [I*]/[I] (hydrolysis constant, K_{hyd}) is often close to unity (i.e. about 50% of the inhibitor molecules contain the reactive site cleaved) at pH 6 where K_{hyd} is pH-independent (Finkenstadt *et al.*, 1974; Siekmann *et al.*, 1988; Otlewski & Zbyryt, 1994). However, there are known examples of natural ovomucoid third domain variants with K_{hyd} in the range 0.4 to 35 (Ardelt & Laskowski, 1991).

(vii) while k_{on} values for proteinase–inhibitor association are typically about 10^6 $M^{-1}s^{-1}$, k_{off} values may differ by many orders of magnitude. The k_{on}* values can also differ

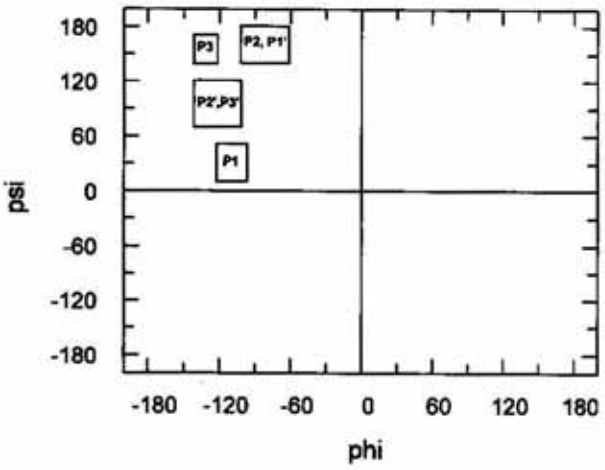

Figure 8. The Ramachandran plot showing ranges of φ and ψ dihedral angles that define canonical conformation of the proteinase binding loop in canonical inhibitors.

The ranges of adopted ϕ and ψ angles are as follows: P_3 ($-140^\circ < \varphi < -120^\circ$; $140^\circ < \psi < 170^\circ$); P_2 ($-100^\circ < \varphi < -60^\circ$; $140^\circ < \psi < 180^\circ$); P_1 ($-120^\circ < \varphi < -95^\circ$; $9^\circ < \psi < 50^\circ$); P_1' ($-100^\circ < \varphi < -60^\circ$; $140^\circ < \psi < 180^\circ$); P_2' ($-140^\circ < \varphi < -100^\circ$; $70^\circ < \psi < 120^\circ$), and P_3' ($-140^\circ < \varphi < -100^\circ$; $70^\circ < \psi < 120^\circ$).

by many orders of magnitude for the interaction of one inhibitor with different proteinases (Ardelt & Laskowski, 1985).

(viii) at high concentration of enzyme and inhibitor the existence of additional unstable loose complexes L, L* and X can be detected by stopped-flow methods (Finkenstadt *et al.*, 1974; Quast *et al.*, 1978).

Proteinase–inhibitor complex

The mode of recognition between serine proteinases and different canonical inhibitors is always very similar. In a stable complex which has been a subject of numerous crystallographic studies, a short antiparallel β-sheet is formed between the P_3 and P_1 residues and the 214–216 (Ser125–Gly127 in subtilisin) segment of the enzyme (Fig. 9). Energetic contribution of one of these intermolecular main chain hydrogen bonds (donated by NH amide of P_1 residue of OMTKY3) has been recently found to be about 1.5 kcal/mole (Lu *et al.*, 1997a). There is an additional antiparallel β-sheet between P_4-P_6 fragment and Tyr104–Gly102 residues in subtilisin complexes which does not exist in chymotrypsin-like enzymes (McPhalen & James, 1988; Takeuchi *et al.*, 1991). Other very impor-

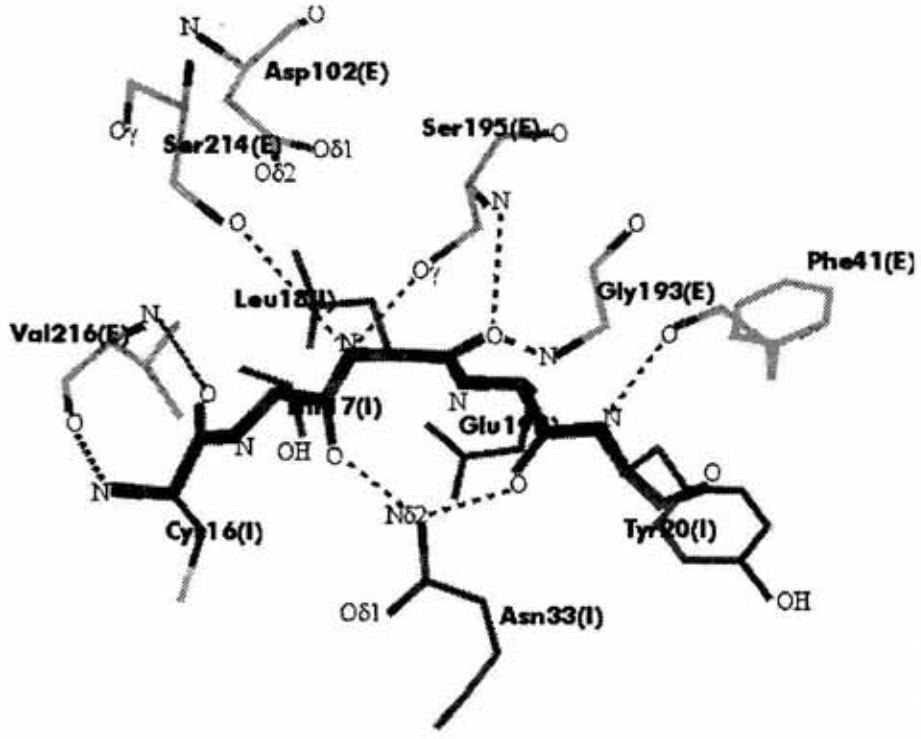

Figure 9. Schematic representation of the canonical inhibition based on the three-dimensional structure of OMTKY3:hNE complex (Bode *et al.*, 1986a).

The inhibitor (shown in bold) binds to the proteinase similarly as to a typical substrate. Several characteristic interactions are shown: (i) an antiparallel β-sheet between segments P_1-P_3 of the inhibitor and 214–216 of the proteinase, (ii) sub-van der Waalas' contact between Ser195 O^γ and the P_1 carbonyl carbon, and (iii) hydrogen bonds from the oxyanion binding hole (NHs of Gly193 and Ser195) to the P_1 carbonyl oxygen.

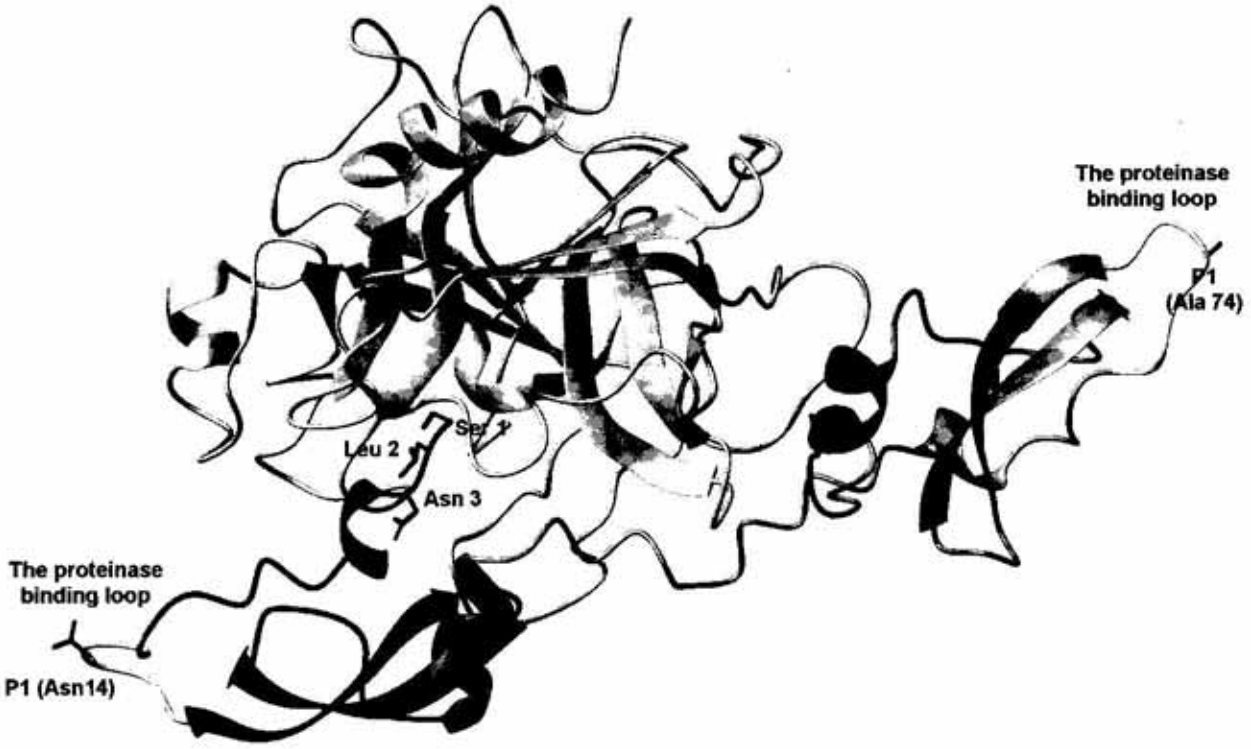

Figure 10. Ribbon diagram of the ornithodorin–thrombin complex (van de Locht *et al.*, 1996).

The inhibitor N-terminal domain (dark grey), C-terminal domain (middle grey) and thrombin (light grey) are shown. The N-terminal domain interacts with the enzyme active site through Ser1-Leu2-Asn3 terminus forming a short parallel β-sheet with thrombin Ser214-Gly219 segment. The C-terminal domain forms three ion pairs and hydrophobic interactions with the fibrinogen binding exosite. The proteinase binding loops of both ornithodorin domains stay away from the enzyme surface.

tant features of the complex include: a short (about 2.7 Å) contact between the P_1 carbonyl carbon and the catalytic serine residue (significantly shorter in rhodniin-bTHRO and MBTI:pTP complexes) and two hydrogen bonds between carbonyl oxygen of P_1 and Gly193/Ser195 amides of the oxyanion binding hole. The reactive site peptide bond remains intact in all crystallographically studied complexes. All the above mentioned hydrogen bonds and the shape complementarity of interacting areas ensure a very similar manner of recognition between different proteinases and inhibitors. In the complex, about 10–17 amino-acid residues on the inhibitor site and 17–29 residues of the proteinase make numerous, mainly van der Waals (typically more than a hundred) and hydrogen bond (about 8–14) interactions. The total area of the components of the two complexes buried in the interface is about 1200–2000 $Å^2$. As concluded, from NMR relaxation parameters of free inhibitors (Peng & Wagner, 1992; Shaw *et al.*, 1995; Liu *et al.*, 1996b), the proteinase binding loop often belongs to the most disordered part of free inhibitor, and becomes significantly rigidified in the complex. However, the loops of anistasin (Lapatto *et al.*, 1997) and BPTI (Wlodawer *et al.*, 1984) are also well defined in uncomplexed state. There are no significant conformational changes on either enzyme or inhibitor side accompanying complex formation.

In contrast, in the trypsinogen–inhibitor complexes major structural rearrangements are observed in the zymogen binding site

Figure 11. Ribbon presentation of the complex of the heavy chain of factor Xa–rTAP (Wei *et al.*, 1998).

The N-terminus of r-TAP is located in the active site of factor Xa with the side chain of Tyr1 located in the S_1 pocket and Arg3 located at the aryl binding pocket. The C-terminal helix of inhibitor forms additional contacts with factor Xa. Similarly as in the case of ornithodorin-thrombin complex (Fig. 10), the P_1 side chain does not form an interaction with the proteinase.

(Huber & Bode, 1978). The organization of the activation domain in the complex with inhibitor is remarkably similar to that observed in active enzyme. The association constant is about 10^7-fold lower than for the active enzyme (Bode, 1979; Antonini *et al.*, 1983), indicating that about 10 kcal/mole of free energy is required to force cooperatively the activation domain into the active, ordered conformation. Despite inherently low activity, the standard mechanism works also for trypsinogen, which is able to resynthesise the reactive site peptide bond of inhibitor (Zbyryt & Otlewski, 1991).

Position P_1 is of particular importance for the proteinase–inhibitor association energy. With the exception of Trp, Ile and Cys, all amino acids have been observed at this position in determined sequences of inhibitors representing different families (Laskowski, 1986). P_1 Gly and particularly P_1 Pro are very bad residues for most of the tested proteinases (Lu *et al.*, 1997b; Krowarsch *et al.*, 1999). Also charged P_1 side chains of Asp and Glu (but not their uncharged forms), when placed in hydrophobic S_1 pockets strongly oppose complex formation (Qasim *et al.*, 1995). The P_1 side chain is fully exposed in all free inhibitor structures and becomes imbedded in the S_1 pocket upon complex formation. It can form up to 50% of the interface contact area and provide more than 50% of association energy as deduced from cognate P_1 – Gly P_1 comparisons (Lu *et al.*, 1997b; Qasim *et al.*, 1997). Cognate P_1 side chains enter the S_1 pocket preserving optimal angles (Huang *et*

Figure 12. Ribbon drawing of the three-dimensional structure of the reactive site hydrolyzed human α_1-antitrypsin (tetragonal form) (Löbermann *et al.*, 1984).

The newly liberated chain termini Met358 and Ser359 are separated by 70 Å. β-Sheet A is located in front of the picture in vertical orientation with s4A strand inserted antiparalelly between s5A and s3A.

al., 1995; Helland *et al.*, 1999a). Improperly matched P_1-S_1 interaction in terms of size, shape, charge, polarity or branching of the P_1 side chain leads to severe effects on the association energy (Beckmann *et al.*, 1988; Kojima *et al.*, 1991; Qasim *et al.*, 1997; Helland *et al.*, 1999a). Also alanine-scanning mutagenesis of BPTI (Castro & Anderson, 1996) and theoretical calculations on proteinase–inhibitor interaction (Krystek *et al.*, 1993) clearly reveal a dominant role of P_1 residue. Since this residue occupies a central part of the canonical loop its substitutions with different amino acids in inhibitor families provides similar energetic effects on binding to serine proteinases, a phenomenon called interscaffolding additivity (Qasim *et al.*, 1997; Krowarsch *et al.*, 1999). Interestingly, in several cases where extensive contacts between enzyme and inhibitor occur also at a remote site, non-cognate side chains are found at P_1 position (ecotin – P_1 Met, rhodniin – P_1 His). The plot of the substrate transition state energy $\log(k_{cat}/K_m)$ *versus* enzyme–inhibitor association energy $\log(K_a)$ determined for a set of P_1 oligopeptide substrates and protein inhibitors is a straight line with a slope not far from unity, suggesting that interactions within the S_1 pocket are not changed as the reaction proceeds from enzyme–inhibitor complex to transition state (Kojima *et al.*, 1991; Lu *et al.*, 1997b; Polanowska *et al.*, 1998).

Free energies of individual interactions between residues forming the loop and the proteinase are often found to be additive (Wells, 1990; Qasim *et al.*, 1997). This offers a possibility of creating strong inhibitors even for highly specific enzymes through careful design of multiple mutants (Komiyama *et al.*, 1991; Lu *et al.*, 1993). There are also reports of

Figure 13. Three-dimensional structure of the active form of human α_1-antitrypsin (tetragonal form) (Elliott *et al.*, 1996).

The reactive site loop of the inhibitor fits into the active site of trypsin without steric conflicts. The loop superimposes well with the canonical loops of Bowman-Birk inhibitor PI-II and hPSTI (rmsd for the Cα atoms is about 0.6 Å).

successful applications of combinatorial phage-displayed libraries based on BPTI, APPI and TFPI inhibitors to create potent variants of closely consensus sequence (Roberts *et al.*, 1992; Dennis & Lazarus, 1994a, b; Markland *et al.*, 1996).

In recent years two interesting variations of the canonical interaction have been reported. Rhodniin is a specific inhibitor of thrombin composed of two Kazal-type domains. Its first domain interacts through the canonical proteinase binding loop with the active site of thrombin in a typical way (van de Locht *et al.*, 1995). The C-terminal domain, due to accumulation of negative charges, binds to the fibrinogen recognition exosite through dominant electrostatic interactions; only two direct hydrogen bonds are formed, however. These electrostatic interactions are reminiscent of the non-canonical hirudin–thrombin interaction and the complex can be considered as characterized by both canonical and non-canonical recognition. The canonical interaction through the second domain is prevented due to a single amino acid insertion and distortion of the binding loop. A strategy of linking two proteins that independently interact at separate binding sites of proteinase was successfully applied to generate a potent inhibitor of factor VIIa through fusion of APPI domain and a soluble tissue factor variant (Lee *et al.*, 1997).

Canonical inhibitors do not inhibit thrombin due to the narrow and deep canyon-like active site cleft which is too narrow for the broad canonical loop. Nevertheless, it was possible to

Figure 14. The structure of latent antithrombin (Carrell *et al.*, 1994).

This form crystallizes as an active:latent dimer. The active molecule has an exposed reactive site loop with initial entry of two residues into the β-sheet A. The latent molecule which is shown on the Figure has a loop totally incorporated (shown as a dark grey β-strand). The two molecules are bridged by the reactive site loop of the active form which has replaced a strand from another active:latent dimer in the latent molecule. The structure reveals unusual mobility of the reactive site loop. It also clearly suggests the mode of polymerization which occurs spontaneously with the Z mutant (Glu342Lys) of α_1PI and leads to accumulation of the polymerized inhibitor in the liver.

construct a potent inhibitor of thrombin based on canonical inhibitor LDTI. The design scheme comprised addition of an acidic C-terminal tail to facilitate interactions at fibrinogen exosite and trimming the binding loop region through multiple substitutions to fit the narrow active site of thrombin (Morenweiser *et al.*, 1997). Also, the engineering of thrombin active site structure through a single E192Q mutation significantly facilitated complex formation with BPTI through rearrangement of the surface loops, particularly 60-loop (van de Locht *et al.*, 1997).

Ecotin illustrates an even more complicated extension of the canonical interaction (Fig. 2). First, the inhibitor exists in solution as a dimer which binds two proteinase molecules, each at two distinct areas. The first region involves the reactive site loop (the 80s loop) and the 50s loop. The second area includes two loops: the 60s loop and the 100s loop from the second ecotin molecule. The total buried area of ecotin–proteinase is about 2800 Å^2, 100% larger than for typical canonical inhibitors, and 50% larger than for non-canonical inhibitors of thrombin. The P_1 residue of ecotin is Met84 which is able to bind in S_1 pockets of serine proteinases of very different specificities, including: trypsin, chymotrypsin, chymase, pancreatic and leukocyte elastases, plasma kallikrein, crab collagenase, factor X_a, and XII_a (McGrath *et al.*, 1995). The side chain of Met due to its flexibility adopts different conformations in the S_1 pockets of trypsin, chymotrypsin and collagenase (McGrath *et al.*, 1995) what partially explains panspecific properties of the inhibitor. The second and perhaps more important source of its broad specificity are the strong interactions at two secondary binding loops which act cooperatively, and not additively, with each other and with substitutions at P_1 site and dimer interface (Yang *et al.*, 1998). Surprisingly, single mutations at P_1 site have but

Table 2. Three-dimensional structures of serpins determined by X-ray crystallography.

Table includes all important serpin structures and lists serpin and proteinase abbreviations used in the paper.

Structure	Abbreviation	PDB code	Method (X-ray)	Reference
Human α_1-antitrypsin (tetragonal form) (reactive site hydrolyzed)	hα_1PI* (I)	7API	3.0 Å	Engh *et al.*, 1989
hα_1PI mutant	hα_1PI (F51L)	1PSI	2.9 Å	Elliott *et al.*, 1996
hα_1PI mutant (F51L,T68A,T59A,A70G, M374I, S381A,K387R)	Hepta hα_1PI	1ATU	2.7 Å	Ryu *et al.*, 1996
Horse leukocyte elastase inhibitor (reactive site hydrolyzed)	hrLEI*	1HLE	1.9 Å	Baumann *et al.*, 1991b
Human α_1-antichymotrypsin mutant (A349G,A350T,T356I,L357P,L358M, A360I,L361P,V368T)	hα_1-ACT-P3-P3′		2.5 Å	Wei *et al.*, 1994
hα_1-ACT* mutant	hα_1-ACT* (A349R)	1AS4	2.1 Å	Lukacs *et al.*, 1998
Chicken ovalbumin	chOVA	1OVA	1.9 Å	Stein *et al.*, 1990; 1991
Ovalbumin (reactive site hydrolyzed)	PLA		2.8 Å	Wright *et al.*, 1990
Bovine antithrombin III (reactive site hydrolyzed)	bATIII*	1ATT	3.2 Å	Delarue *et al.*, 1990; Mourey *et al.*, 1993
hATIII	hATIII	1ANT	2.6 Å	Wardell *et al.*, 1993
hATIII (active:latent dimer)	hATIII	2ANT	2.6 Å	Skinner *et al.*, 1997
hATIII:hATIII* (latent:cleaved dimer)	hATIII:hATIII*	1ATH	3.2 Å	Schreuder *et al.*, 1994
hATIII:pentasaccharide	hATIII: pentasaccharide	1AZX	2.9 Å	Jin *et al.*, 1997
hATIII:P_{14}-P_3 peptide	hATIII:P_{14}-P_3	1BR8	2.9 Å	Skinner *et al.*, 1998
Human plasminogen activator inhibitor 1 (latent)	hPAI-1		2.6 Å	Mottonen *et al.*, 1992
hPAI-1 (N150H,K154T,Q319L,M354I)	hPAI-1 quadruple mutant	1B3K	3.0 Å	Sharp *et al.*, 1999
hPAI-mutant (reactive site hydrolyzed)	hPAI-1 (A335P)*	9PAI	2.7 Å	Aertgeerts *et al.*, 1995
hPAI-2 mutant (residues 66-98 deleted)	hPAI-2	1BY7	2.0 Å	Harrop *et al.*, 1999
Serpin 1K from *Manduca sexta*	1K	1SEK	1.2 Å	Li *et al.*, 1999

neglible effects on association energy, as compared to effects of mutations of typical canonical inhibitors.

NON-CANONICAL INTERACTIONS

In recent years also non-canonical complexes between protein inhibitors and serine proteinases have been studied by X-ray crystallography (Table 1). These inhibitors origin from blood sucking organisms and specifically block enzymes of the blood clotting cascade, particularly thrombin or factor Xa. The interaction is mediated mainly through inhibitor N-terminus, which is disordered in solution and rearranges upon binding in the active site of an enzyme (Szyperski *et al.*, 1992a, b).

The N-terminus binds through the parallel β-sheet which is of somewhat different length. The detailed interactions of the three N-terminal residues are different in non-canonical complexes. There are also extensive secondary interactions which provide an additional buried area and contribute significantly to the strength and specificity of interaction. In the studied cases there is a two-step kinetics of association – the initial slow binding step occurs at the secondary binding site, then the N-terminus locks in the active site of proteinase.

The first recognized inhibitor of this class was hirudin – a 66 amino-acid residues protein from the saliva of medical leech. Both for hirudin in solution and for its complexes the structure is known. There are several key features which distinguish the hirudin–thrombin recognition from the canonical interaction. The enzyme–inhibitor contacts comprise 27 out of 65 hirudin residues (Rydel *et al.*, 1990; 1991). The active site of thrombin is blocked not by the loop segment but by insertion of the three N-terminal residues in a parallel β-sheet arrangement to S_1-S_3 sites, in contrast to antiparallel orientation observed for the canonical inhibitors. Neither catalytic Ser195 nor the S_1 pocket are specifically blocked by the inhibitor. The α-amino group of Ile1 forms hydrogen bonds with hydroxyl of Ser195 and the carbonyl carbon of Ser214; Thr3 does not enter the S_1 pocket to make a hydrogen bond with Asp189 at the bottom of the pocket. Nevertheless, the complementarity of interacting surfaces allows formation of hydrogen bond and ion pair interactions, many of which are mediated through water molecules. There is an important additional region of contact between the extended C-terminal tail of hirudin and the fibrinogen recognition exosite. The hirudin tail starting from residue 49, which is disordered in solution (Folkers *et al.*, 1989), interacts through multiple electrostatic interactions and also van der Waals contacts. The electrostatic component of hirudin-thrombin association allows for an extremely fast (k_{on} = $1 \times 10^9\ M^{-1}\ s^{-1}$) and strong ($K_i = 10^{-14}$ M) interaction (Ascenzi *et al.*, 1992).

Two other non-canonical inhibitors of coagulation proteinases show, surprisingly, a scaffold similar to an archetypical canonical inhibitor – BPTI. The ornithodorin from the soft tick contains two BPTI-like domains containing insertion/deletion in the binding loop segment which lead to major distortions of both binding loops (van de Locht *et al.*, 1996). In fact, these binding loops do not contact the proteinase (Fig. 10). Similarly as in the hirudin–thrombin complex, the N-terminal tail penetrates into the active site and forms a parallel β-sheet with the thrombin Ser214–Gly219 segment. There are also several other regions contacting thrombin which provide together a surface of 1100 $Å^2$. The C-terminal domain contacts cover 700 $Å^2$ and include three salt bridges formed in the fibrinogen exosite area.

TAP is another anticoagulant protein found in the soft tick which is a strong inhibitor of factor Xa (Waxman *et al.*, 1990; Antuch *et al.*, 1994). Like in the hirudin–thrombin interaction, TAP interacts through the N-terminus with the active site of proteinase (Wei *et al.*, 1998). Conversely to expected preferences, phenol ring of Tyr1 is bound in the S_1 pocket and Arg3 interacts with the aryl binding site (Fig. 11). The secondary binding determinant comprises C-terminal helix of TAP which forms electrostatic interactions with the autolysis loop of factor Xa.

Finally, triabin, a 142-residue protein from the saliva of triatomine bug, is an unusual inhibitor of thrombin which only slightly reduces its activity toward low molecular mass substrates. Crystal structure of the triabin–thrombin complex shows strong interactions exclusively through the fibrinogen exosite (Fuentes-Prior *et al.*, 1997). Although complexation occurs *via* the same area of thrombin as in the case of rhodniin and ornithodorin inhibitors, the interactions with triabin are almost exclusively hydrophobic in nature, in contrast to the electrostatic interaction de-

scribed above for non-canonical inhibitors. Also, in contrast to the complexes of the latter inhibitors, the active site of triabin-complexed-thrombin is free to act on small substrates.

SERPINS

There are several notable features in which serpins differ from the standard mechanism inhibitors. Serpins are significantly larger proteins (of about 400 residues). The complex structure of serpins enables regulation of their action through association with a variety of cofactors and receptors. Although non-inhibitory serpins are also known (ovalbumin, hormone transporters, peptide hormone precursors), most of the studied serpins are plasma proteins which are targeted toward serine proteinases and thus control critically important processes, such as phagocytosis, coagulation, and fibrinolysis (Table 2).

Serpins contain three β-sheets (A–C) and nine α-helices (A–I). The proteinase binding loop of serpins, located in the C-terminal part of the molecule, comprises about 30 residues, and, due to inherent flexibility, can adopt a number of different conformations. The first structure reported for a member of the family was the reactive site (Met358–Ser359) cleaved form of hα_1PI (Löbermann, 1984). In the structure, the P_3-P_{15} segment of the binding loop is inserted as the central strand (s4A) in the β-sheet A, while the twisted β-sheet C contains the downstream segment of the cleaved binding loop as its edge strand s1C (Fig. 12). The newly released N- and C-termini in hα_1PI* are separated in space by 70 Å, strongly suggesting that resynthesis of the bond is impossible. Similar organization of the cleaved molecule was later observed in the case of other serpins: bATIII* (Mourey *et al.*, 1993; Schreuder *et al.*, 1994), hα_1ACT* (Baumann *et al.*, 1991a), hrLEI* (Baumann *et al.*, 1991b), hPAI-1 (A335P)* (Aertgeerts *et al.*, 1995). Although the three-dimensional structure for the serpin–proteinase complex so far has not been reported, the huge conformational change accompanying the cleavage reaction implies that the mechanism of serpin action is different from the standard mechanism. In non-inhibitory chOVA, cleavage of the reactive loop does not lead to insertion of the released segments (Wright *et al.*, 1990; Wright & Scarsdale, 1995), again suggesting that strand annealing is relevant to the inhibitory mechanism.

Intact serpins show a surprisingly high binding loop flexibility. The loop can be fully inserted into the A β-sheet, in the structure of uncleaved serpins, as found in hPAI-1 (Mottonen *et al.*, 1992) and hATIII (Fig. 14) (Carrell *et al.*, 1994; Skinner *et al.*, 1997). This so called latent state can be observed not only in crystallized dimers of serpins (one molecule latent and one active), but can also be initiated by exposure to mild denaturing conditions in other serpins, like α_1PI (Lomas *et al.*, 1995). Moreover, spontaneous transition to latent state is implicated in the physiological action of PAI-1 that enables this serpin to exist in plasma in inactive state.

Conformation of the binding loop is also different among intact, non-latent forms of different serpins. The structures of hα_1PI (Fig. 13) (Elliott *et al.*, 1996) and hα_1-ACT (Wei *et al.*, 1994) show no insertion, while hATIII (Schreuder *et al.*, 1994; Carrell *et al.*, 1994) has a two-residue insertion. However, upon complexation with pentasaccharide heparin, which is known to give a 300-fold increase in inhibitory activity, the loop of hATIII becomes fully exposed (Jin *et al.*, 1997). The loop conformation also varies among intact serpins: from a distorted α-helix in hα_1-ACT to an almost canonical form observed in hα_1PI, suggesting that initial serpin–proteinase recognition might be similar to that found in canonical inhibitor complexes.

Synthetic exogenous peptides with the sequence of P_2-P_{14} segment can spontaneously incorporate as strand 4 of β-sheet A in respec-

tive binary complexes of α_1PI (Schulze *et al.*, 1990) and ATIII (Björk *et al.*, 1992). The stability of the reactive site cleaved and latent serpins and also of serpin-peptide binary complexes is much higher than that of native, uncleaved form (Bruch *et al.*, 1988) this results from reorganization of the five stranded β-sheet A in native molecule to a six stranded, predominantly antiparallel form. Contrary to the latent, non-inhibitory form, the binary complex is a substrate for its target proteinase, since upon cleavage this complex cannot incorporate the binding loop segment into β-sheet structure.

It follows that the active, inhibitory state of serpins has a mobile and exposed binding loop and exists as a metastable folding intermediate of relatively high energy. Non-inhibitory serpins, like chOVA, do not show the conformational change accompanying the cleavage reaction (Stein *et al.*, 1989). Recent mutational studies on α_1PI have identified several unfavourable hydrophobic interactions in its central core which appear to create strains in native wild type inhibitor and act as a sheet-opening trigger (Ryu *et al.*, 1996). Nevertheless, an engineered variant of α_1PI with improved hydrophobic core interactions and high stability (comparable to that of chOVA) still preserved inhibitory properties (Lee *et al.*, 1998).

Studies on both natural, disfunctional variants (Stein & Carrell, 1995; Carrell *et al.*, 1997) and engineered mutants (Hood *et al.*, 1994; Tucker *et al.*, 1995) of serpins revealed that the residues in P_{10}-P_{15} segment (the hinge region) are essential for inhibitory activity. In natural serpins this region is conserved and contains small side chains which are able to form a flexible turn. A current working model of serpin action assumes two step complex formation: rapid reversible canonical recognition, followed by cleavage reaction which produces a stable acyl-enzyme complex (Lawrence, 1997; Stone et al.,1997). In the second step a rapid insertion of the loop into β-sheet A at least up to the position P_9 leads to formation of a stable complex (Shore *et al.*, 1995). A critical factor for effective formation of the complex is the rate of loop insertion. If insertion of the binding loop is blocked by an exogenously added peptide or if the rate of full hydrolysis of the reactive site (the deacylation rate) can be attained before loop insertion into β-sheet, the serpin will behave as a substrate. If the insertion rate is faster, the complex will be stabilised. It is not clear, however, what is the driving force of the described molecular events: to what extent binding of an enzyme induces the insertion of the loop and when hydrolysis of the P_1-P_1' bond does occur.

REFERENCES

Aertgeerts, K., De Bondt, H., De Ranter, C.J. & Declerck, P.J. (1995) Mechanisms contributing to the conformational and functional flexibility of plasminogen activator inhibitor-1. *Nature Struct. Biol.* **2**, 891–897.

Antonini, E., Ascenzi, P., Bolognesi, M., Gatti, G., Guarneri, M. & Menegatti, E. (1983) Interaction between (pro)enzyms and Kazal and Kunitz inhibitors. *J. Mol. Biol.* **165**, 543–558.

Antuch, W., Berndt, K.D., Chávez, M.A., Delfín, J. & Wüthrich, K. (1993) The NMR solution structure of a Kunitz-type proteinase inhibitor from the sea anemone *Stichodactyla helianthus*. *Eur. J. Biochem.* **212**, 675–684.

Antuch, W., Güntert, P., Billeter, M., Hawthorne, T., Grossenbacher, H. & Wüthrich, K. (1994) NMR solution structure of the recombinant tick anticoagulant protein (rTAP), a factor Xa inhibitor from the tick *Ornthodoros moubata*. *FEBS Lett.* **352**, 251–257.

Apostoluk, W. & Otlewski, J. (1998) Variability of the canonical loop conformations in serine proteinases inhibitors and other proteins. *Proteins: Struct. Funct. Genet.* **32**, 459–474.

Ardelt, W. & Laskowski, M., Jr. (1983). Thermodynamics and kinetics of the hydrolysis and resynthesis of the reactive site peptide bond in turkey ovomucoid third domain by asper-

gillopeptidase B. *Acta Biochim. Polon.* **30**, 115–126.

Ardelt, W. & Laskowski, M., Jr. (1985) Turkey ovomucoid third domain inhibits eight different serine proteinases of varied specificity on the same ... Leu18 – Glu19 ... reactive site. *Biochemistry* **24**, 5313–5320.

Ardelt, W. & Laskowski, M., Jr. (1991) Effect of single amino acid replacements on the thermodynamics of the reactive site peptide bond hydrolysis in ovomucoid third domain. *J. Mol. Biol.* **220**, 1041–1053.

Ascenzi, P., Amiconi, G., Coletta, M., Lupidi, G., Menegatti, E., Onesti, S. & Bolognesi, M. (1992) Binding of hirudin to α,β and γ-thrombin. A comparative kinetic and thermodynamic study. *J. Mol. Biol.* **225**, 177–184.

Baumann, U., Huber, R., Bode, W., Grosse, D., Lesjak, M. & Laurell, C. B. (1991a) Crystal structure of cleaved human α_1-antichymotrypsin at 2.7 Å resolution and its comparison with other serpins. *J. Mol. Biol.* **218**, 595–606.

Baumann, U., Bode, W., Huber, R., Travis, J. & Potempa, J. (1991b) Crystal structure of cleaved equine leucocyte elastase inhibitor determined at 1.95 Å resolution. *J. Mol. Biol.* **226**, 1207–1218.

Beckmann, J., Mehlich, A., Schröder, W., Wenzel, H.R. & Tschesche, H. (1988) Preparation of chemically 'mutate' aprotinin homologues by semisynthesis. P_1 substitutions change inhibitory specificity. *Eur. J. Biochem.* **176**, 675–682.

Beeser, S.A., Goldenberg, D.P. & Oas, T.G. (1997) Enhanced protein flexibility caused by a destabilizing amino acid replacement in BPTI. *J. Mol. Biol.* **269**, 154–164.

Behnke, C.A., Yee, V.C., Trong, I.L., Pedersen, L.C., Stenkamp, R.E., Kim, S.S., Reeck, G.R. & Teller, D.C. (1998) Structural determinants of the bifunctional corn Hageman factor inhibitor: X-ray crystal structure at 1.95 Å resolution. *Biochemistry* **37**, 15277–15288.

Berndt, K.D., Güntert, P., Orbons, L.P. & Wüthrich, K. (1992) Determination of a high quality nuclear magnetic resonance solution structure of the bovine pancreatic trypsin inhibitor and comparison with three crystal structures. *J. Mol. Biol.* **227**, 757–775.

Betzel, C., Dauter, Z., Genov, N., Lamzin, V., Navaza, J., Schnebli, H.P., Visanji, M. & Wilson, K.P. (1993) Structure of the proteinase inhibitor eglin c with hydrolysed reactive center at 2.0 Å resolution. *FEBS Lett.* **317**, 185–188.

Björk, I., Ylinenjärvi, K., Olson, S.T. & Bock, P.E. (1992) Conversion of antithrombin from an inhibitor of thrombin to a substrate with reduced heparin affinity and enhanced conformational stability by binding of a tetradecapeptide corresponding to the P1-P14 region of the putative reactive bond loop of the inhibitor. *J. Biol. Chem.* **267**, 1976–1982.

Bode, W. (1979) The transition of bovine trypsinogen to a trypsin-like state upon strong ligand binding. II. The binding of the pancreatic trypsin inhibitor and of isoleucine-valine and of sequentially related peptides to trypsinogen and to *p*-guanidinobenzoate-trypsinogen. *J. Mol. Biol.* **127**, 357–374.

Bode, W., Epp, O., Huber, R., Laskowski, M., Jr. & Ardelt, W. (1985) The crystal and molecular structure of the third domain of silver pheasant ovomucoid (OMSVP3). *Eur. J. Biochem.* **147**, 387–395.

Bode, W., Schwager, P. & Huber, R. (1978) The transition of bovine trypsinogen to a trypsin-like state upon ligand binding. The refined crystal structures of bovine trypsinogen-pancreatic trypsin inhibitor complex and of its ternary complex with the Ile–Val at 1.9 Å resolution. *J. Mol. Biol.* **118**, 99–112.

Bode, W., Wei, A.-Z., Huber, R., Meyer, E., Travis, J. & Neuman, S. (1986a) X-ray crystal structure of the complex of human leukocyte elastase (PMN elastase) and the third domain of turkey ovomucoid inhibitor. *EMBO J.* **5**, 2453–2458.

Bode, W., Papamokos, E., Musil, D., Seemüller, U. & Fritz, H. (1986b) Refined 1.2 Å crystal structure of the complex formed between subtilisin Carlsberg and the inhibitor eglin c. *EMBO J.* **5**, 813–818.

Bode, W., Greyling, H.J., Huber, R., Otlewski, J. & Wilusz, T. (1989) The refined 2.0 Å X-ray crystal structure of the complex formed between bovine β-trypsin and CMTI-I, a trypsin inhibitor from squash seeds (*Cucurbita maxima*): Topological similarity of the squash seed inhibitors with the carboxypeptidase A inhibitor from potatoes. *FEBS Lett.* **242**, 285–292.

Bode, W. & Huber, R. (1992) Natural protein proteinase inhibitors and their interaction with proteinases. *Eur. J. Biochem.* **204**, 433–451.

Bolognesi, M., Gatti, G., Menegatti, E., Guarneri, M., Marquart, M., Papamokos, E. & Huber, R. (1982) Three-dimensional structure of the complex between pancreatic secretory trypsin inhibitor (Kazal type) and trypsinogen at 1.8 Å resolution. *J. Mol. Biol.* **162**, 839–868.

Bolognesi, M., Pugliese, L., Gatti, G., Frigero, F., Coda, A., Antolini, L., Schnebli, H.P., Menegatti, E., Amiconi, G. & Ascenzi, P. (1990) X-ray crystal structure of the bovine α-chymotrypsin/eglin c complex at 2.6 Å resolution. *J. Mol. Recogn.* **3**, 163–168.

Bruch, M., Weiss, V. & Engel, J. (1988) Plasma serine proteinase inhibitors (serpins) exhibit major conformational changes and a large increase in conformational stability upon cleavage at their reactive sites. *J. Biol. Chem.* **263**, 16626–16630.

Burgering, M.J.M., Orbons, L.P.M., van der Doelen, A., Mulders, J., Theunissen, H.J.M., Grootenhuis, P.D.J., Bode, W., Huber, R. & Stubbs, M.T. (1997) The second Kunitz domain of human tissue factor pathway inhibitor: Cloning, structure determination and interaction with factor Xa. *J. Mol. Biol.* **269**, 395–407.

Cai, M., Gong, Y., Kao, J.L.-F. & Krishnamoorthi, R. (1995a) Three-dimensional solution structure of *Cucurbita maxima* trypsin inhibitor-V determined by NMR spectroscopy. *Biochemistry* **34**, 5201–5211.

Cai, M., Gong, Y., Prakash, O. & Krishnamoorthi, R. (1995b) Reactive-site hydrolyzed *Cucurbita maxima* trypsin inhibitor-V: Function, thermodynamic stability, and NMR solution structure. *Biochemistry* **34**, 12088–12094.

Cai, M., Huang, Y., Prakash, O., Wen, L., Dunkelbarger, S.P., Huang, J.K., Liu, J. & Krishnamoorthi, R. (1996) Differential modulation of binding loop flexibility and stability by Arg50 and Arg52 in *Cucurbita maxima* trypsin inhibitor-V deduced by trypsin-catalyzed hydrolysis and NMR spectroscopy. *Biochemistry* **35**, 4784–4794.

Carrell, R.W., Stein, P.E., Fermi, G. & Wardell, M.R. (1994) Biological implications of a 3 Å structure of dimeric antithrombin. *Structure* **2**, 257–270.

Carrell, R., Lomas, D., Stein, P. & Whiststock, J. (1997) Dysfunctional variants and the structural biology of the serpins. *Adv. Exp. Med. Biol.* **425**, 207–222.

Castro, M.J.M. & Anderson, S. (1996) Alanine point-mutations in the reactive region of bovine pancreatic trypsin inhibitor: Effects on the kinetics and thermodynamics of binding to β-trypsin and α-chymotrypsin. *Biochemistry* **35**, 11435–11446.

Chen, Z. & Bode, W. (1983) Refined 2.5 Å X-ray crystal structure of the complex formed by porcine kallikrein A and the bovine pancreatic trypsin inhibitor: Crystallisation, Patterson search, structure determination, refinement, structure and comparison with its components and with the bovine trypsin-pancreatic trypsin inhibitor complex. *J. Mol. Biol.* **164**, 283–311.

Chen, P., Rose, J., Love, R., Wei, C.H. & Wang, B.C. (1992) Reactive sites of an anticarcinogenic Bowman-Birk proteinase inhibitor are similar to other trypsin inhibitors. *J. Biol. Chem.* **267**, 1990–1994.

Chiche, L., Gaboriaud, C., Heitz, A., Mornon, J.-P., Castro, B. & Kollman, P.A. (1989) Use of restrained molecular dynamics in water to determine three dimensional protein structure: Prediction of the three dimensional structure of *Ecballium elaterium* trypsin inhibitor II. *Proteins: Struct. Funct. Genet.* **6**, 405–417.

Chiche, L., Heitz, A., Padilla, A., Le-Nguyen, D. & Castro, B. (1993) Solution conformation of synthetic bis-headed inhibitor of trypsin and carboxypeptidase A: New structural alignment between the squash inhibitor and the potato

carboxypeptidase inhibitor. *Protein Engng.* **6**, 675–682.

Czapinska, H. & Otlewski, J. (1999) Structural and energetic determinants of the S_1 site specificity in serine proteases. *Eur. J. Biochem.* **260**, 571–595.

Dattagupta, J.K., Podder, A., Chakrabarti, C., Sen, U., Mukhopadhyay, D., Dutta, S.K. & Singh, M. (1999) Refined crystal structure (2.3 Å) of a double-headed winged bean alpha-chymotrypsin inhibitor and location of its second reactive site. *Proteins* **35**, 321–331.

Dauter, Z., Genov, N., Pipon, N., Wilson, K.S. & Betzel, C. (1991) Complex between the subtilisin from a mesophilic bacterium and the leech inhibitor eglin-c. *Acta Cryst.* **B47**, 707–730.

Delarue, M., Samama, J.-P., Mourey, J.-P. & Moras, D. (1990) Crystal structure of bovine antithrombin III. *Acta Crystallog.* **B46**, 550–556.

Dennis, M.S. & Lazarus, R.A. (1994a) Kunitz domain inhibitors of tissue factor – factor VIIa: I. Potent inhibitors selected from libraries by phage display. *J. Biol. Chem.* **269**, 22129–22136.

Dennis, M.S. & Lazarus, R.A. (1994b) Kunitz domain inhibitors of tissue factor – factor VIIa: II. Potent and specific inhibitors by competitive phage selection. *J. Biol. Chem.* **269**, 22137–22144.

Elliott, P.R., Lomas, D.A., Carrell, R.W. & Abrahams, J.P. (1996) Inhibitory conformation of the reactive loop of alpha 1-antitrypsin. *Nature Struct. Biol.* **3**, 676–681.

Engh, R., Lobermann, H., Schneider, M., Wiegand, G., Huber, R. & Laurell, C.B. (1989) The S variant of human alpha 1-antitrypsin, structure and implications for function and metabolism. *Protein Engng.* **2**, 407–415.

Estell, D.A., Wilson, K.A. & Laskowski, M., Jr. (1980) Thermodynamics and kinetics of the hydrolysis of the reactive-site peptide bond in pancreatic trypsin inhibitor (Kunitz) by *Dermasterias imbricata* trypsin 1. *Biochemistry* **19**, 131–137.

Finkenstadt, W.R. & Laskowski, M., Jr. (1967) Resynthesis by trypsin of the cleaved peptide bond in modified soybean trypsin inhibitor. *J. Biol. Chem.* **242**, 771–773.

Finkenstadt, W.R., Hamid, M.A., Mattis, J.A., Schrode, J.A., Sealock, R.W. & Laskowski, M., Jr. (1974) Kinetics and thermodynamics of the interaction of proteinases with protein inhibitors. *Bayer-Symposium V* (Fritz, H., Tschesche, H., Greene, L.J. & Truscheit, E. eds.) pp. 389–411, Springer-Verlag, Berlin.

Folkers, P.J.M., Clore, G.M., Driscoll, P.C., Dodt, J., Khler, S. & Gronenborn, A.M. (1989) Solution structure of recombinant hirudin and the Lys-47-Glu mutant: A nuclear magnetic resonance and hybrid distance geometry-dynamical simulated annealing study. *Biochemistry* **28**, 2601–2617.

Francart, C., Dauchez, M., Alix, A.J.P. & Lippens, G. (1997) Solution structure of R-elafin, a specific inhibitor of elastase. *J. Mol. Biol.* **268**, 666–677.

Fuentes-Prior, P., Noeske-Jungblut, C., Donner, P., Schleuning, W.-D., Huber, R. & Bode, W. (1997) Structure of thrombin complex with triabin, a lipocalin-like exosite-binding inhibitor derived from a triatomine bug. *Proc. Natl. Acad. Sci. U.S.A.* **94**, 11845–11850.

Fujinaga, M., Read, R.J., Sielecki, A., Ardelt, W., Laskowski, M., Jr. & James, M.N.G. (1982) Refined crystal structure of the molecular complex of *Streptomyces griseus* protease B, a serine protease, with the third domain of the ovomucoid inhibitor from turkey. *Proc. Natl. Acad. Sci. U.S.A.* **79**, 4868–4872.

Fujinaga, M., Sielecki, A.R., Read, R.J., Ardelt, W., Laskowski, M., Jr. & James, M.N.G. (1987) Crystal and molecular structures of the complex of α-chymotrypsin with its inhibitor turkey ovomucoid third domain at 1.8 Å resolution. *J. Mol. Biol.* **195**, 397–418.

Gourinath, S., Srinisvasan, A. & Singh, T.P. (1999) Structure of the bifunctional inhibitor of trypsin and α-amylase from ragi seeds at 2.9 Å resolution. *Acta Cryst.* **D55**, 25–30.

Grasberger, B.L., Clore, G.M. & Gronenborn, A.M. (1994) High-resolution structure of Ascaris trypsin inhibitor in solution: Direct ev-

idence for a pH-induced conformational transition in the reactive site. *Structure* **2**, 669–678.

Greenblatt, H.M., Ryan, C.A. & James, M.N.G. (1989) Structure of the complex of *Streptomyces griseus* proteinase B and polypeptide chymotrypsin inhibitor-1 from Russet Burbank potato tubers at 2.1 Å resolution. *J. Mol. Biol.* **205**, 201–225.

Gros, P., Teplyakov, A.V. & Hol, W.G.J. (1992) Effects of eglin-c binding to thermitase: three-dimensional structure comparison of native thermitase and thermitase eglin-c complexes. *Proteins: Struct. Funct. Genet.* **12**, 63–70.

Grütter, M.G., Fendrich, G., Huber, R. & Bode, W. (1988) The 2.5 Å X-ray crystal structure of the acid-stable proteinase inhibitor from human mucous secretions analysed in its complex with bovine α-chymotrypsin. *EMBO J.* **7**, 345–351.

Grütter, M.G., Priestle, J.P., Rahuel, J., Grossenbacher, H., Bode, W., Hofsteenge, J. & Stone, S.R. (1990) Crystal structure of the thrombin-hirudin complex: A novel mode of serine protease inhibition. *EMBO J.* **9**, 2361–2365.

Harding, L., Scott, R.H., Kellenberger, C., Hietter, H., Luu, B., Beadle, D.J. & Bermudez, I. (1995) Inhibition of high voltage-activated Ca^{2+} currents from cultured sensory neurones by a novel insect peptide. *J. Rcept. Signal. Transduct. Res.* **15**, 355–364.

Harrop, S.J., Jankova, L., Coles, M., Jardine, D., Whittaker, J.S., Gould, A.R., Meister, A., King, G.C., Mabbutt, B.C. & Curmi, P.M.G. (1999) The crystal structure of plasminogen activator inhibitor 2 at 2.0 Å resolution: Implications for serpin function. *Structure* **7**, 43–54.

Heald, S.L., Tilton, R.F., Jr., Hammond, L.J., Lee, A., Bayney, R.M., Kamarck, M.E., Ramabhadran, T.V., Dreyer, R.N., Davis, G., Unterbeck, A. & Tambutini, P.P. (1991) Sequential NMR resonance assignment and structure determination of the Kunitz-type inhibitor domain of the Alzheimer's β-amyloid precursor protein. *Biochemistry* **30**, 10467–10478.

Hecht, H.J., Szardenings, M., Collins, J. & Schomburg, D. (1991) Three dimensional structure of the complexes between bovine chymotrypsinogen A and two recombinant variants of human pancreatic secretory trypsin inhibitor (Kazal-type). *J. Mol. Biol.* **220**, 711–722.

Hecht, H.J., Szardenings, M., Collins, J. & Schomburg, D. (1992) Three-dimensional structure of a recombinant variant of human pancreatic secretory trypsin inhibitor (Kazal-type). *J. Mol. Biol.* **225**, 1095–1103.

Heitz, A., Chiche, L., Le-Nguyen, D. & Castro, B. (1989) 1H 2D NMR and distance geometry study of the folding of *Ecbalium elaterium* trypsin inhibitor, a member of the squash inhibitor family. *Biochemistry* **28**, 2392–2398.

Heinz, D.W., Priestle, J.P., Rahuel, J., Wilson, K.S. & Grütter, M.G. (1991) Refined crystal structures of subtilisin Novo in complex with wild-type and two mutant eglins. *J. Mol. Biol.* **217**, 353–371.

Heinz, D.W., Hyberts, S.G., Peng, J.W., Priestle, J.P., Wagner, G. & Grütter, M.G. (1992) Changing the inhibitory specificity and function of the proteinase inhibitor eglin c by site-directed mutagenesis: Functional and structural investigation. *Biochemistry* **31**, 8755–8766.

Helland, R., Leiros, I., Berglund, G.I., Willassen, N.P. & Smalas, A.O. (1998) The crystal structure of anionic salmon trypsin in complex with bovine pancreatic trypsin inhibitor. *Eur. J. Biochem.* **256**, 317–324.

Helland, R., Berglund, G.I., Otlewski, J., Apostoluk, W., Andersen, O.A., Willassen, N.P. & Smalas, A.O. (1999a) High resolution crystal structures of three new trypsin-squash inhibitor complexes. Detailed comparison with other trypsins and their complexes. *Acta Cryst.* **D55**, 139–148.

Helland, R., Otlewski, J., Sundheim, O., Dadlez, M. & Smalas, A.O. (1999b) The crystal structures of the complexes between bovine β-trypsin and ten P1 variants of BPTI. *J. Mol. Biol.* **287**, 923–942.

Hipler, K., Priestle, J.P., Rahuel, J. & Grütter, M. (1992) X-ray crystal structure of the serine proteinase inhibitor eglin c at 1.95 Å resolution. *FEBS Lett.* **309**, 139–145.

Holak, T.A., Gondol, D., Otlewski, J. & Wilusz, T. (1989) Determination of the complete three-dimensional structure of the trypsin inhibitor from squash seeds in aqueous solution by nuclear magnetic resonance and a combination of distance geometry and dynamic simulated annealing. *J. Mol. Biol.* **210**, 635–648.

Holak, T.A., Habazettl, J., Oschkinat, H. & Otlewski, J. (1991) Structure of proteins in solution derived from homonuclear three-dimensional NOE-NOE nuclear magnetic resonance spectroscopy. High resolution structure of squash trypsin inhibitor. *J. Am. Chem. Soc.* **113**, 3196–3198.

Hood, D.B., Huntington, J.A. & Gettins, P.G. (1994) α_1-Antiproteinase inhibitor variant T345R. Influence of P14 residue on substrate and inhibitory pathways. *Biochemistry* **33**, 8538–8547.

Huang, Q., Liu, S. & Tang, Y. (1992) Refined 1.6 Å resolution crystal structure of the complex formed between porcine β-trypsin and MCTI-A, a trypsin inhibitor of the squash family. *J. Mol. Biol.* **229**, 1022–1036.

Huang, K., Strynadka, N.C.J., Bernard, V.D. & James, M.N.G. (1994) The molecular structure of the complex of *Ascaris* chymotrypsin/elastase inhibitor with porcine elastase. *Structure* **2**, 669–678.

Huang, K., Anderson, S., Laskowski, M., Jr. & James, M.N.G. (1995) Water molecules participate in proteinase–inhibitor interactions: Crystal structures of Leu18, Ala18 and Gly18 variants of turkey ovomucoid inhibitor third domain complexed with *Streptomyces griseus* proteinase B. *Protein Sci.* **4**, 1985–1997.

Huber, R., Kukla, D., Bode, W., Schwager, P., Bartels, K., Deisenhofer, J. & Steigemann, W. (1974) Structure of the complex formed by bovine trypsin and bovine pancreatic trypsin inhibitor. *J. Mol. Biol.* **89**, 73–101.

Huber, R., Bode, W., Kukla, D., Kohl, U. & Ryan, C.A. (1975) The structure of the complex formed by bovine trypsin and bovine pancreatic trypsin inhibitor. Structure of the anhydro-trypsin–inhibitor complex. *Biophys. Struct. Mech.* **1**, 189–201.

Huber, R. & Bode, W. (1978) Structural basis of the activation and action of trypsin. *Acc. Chem. Res.* **11**, 114–122.

Hurle, M.R., Marks, C.B., Kosen, P.A., Anderson, S. & Kuntz, I.D. (1990) Denaturant-dependent folding of bovine pancreatic trypsin inhibitor mutants with two-intact disulfide bonds. *J. Mol. Biol.* **29**, 4410–4419.

Hyberts, S.G., Goldberg, M.S., Havel, T.F. & Wagner, G. (1992) The solution structure of eglin c based on measurements of many NOEs and coupling constants and its comaprison with X-ray structures. *Protein Sci.* **1**, 736–751.

Hynes, T.R., Randal, M., Kennedy, L.A., Eigenbrot, C. & Kossiakoff, A.A. (1990) X-ray crystal structure of the inhibitor domain of Alzheimer's amyloid β-protein precursor. *Biochemistry* **29**, 10018–10022.

Janin, J. & Chothia, C. (1990) The structure of protein–protein recognition sites. *J. Biol. Chem.* **265**, 16027–16030.

Jin, L., Abrahams, J.P., Skinner, R., Petitou, M., Pike, R.N. & Carrell, R.W. (1997) The anticoagulant activation of antithrombin by heparin. *Proc. Natl. Acad. Sci. U.S.A.* **94**, 14683–14688.

Jones, S. & Thornton, J.M. (1996) Principles of protein–protein interactions. *Proc. Natl. Acad. Sci. U.S.A.* **93**, 13–20.

Kohfeld, E., Göhring, W., Mayer, U., Zweckstetter, M., Holak, T.A., Chu, M.-L. & Timpl, R. (1996) Conversion of the Kunitz-type module of collagen VI into a highly active trypsin inhibitor by site-directed mutagenesis. *Eur. J. Biochem.* **238**, 333–340.

Kojima, S., Nishiyama, Y., Kumagai, I. & Miura, K. (1991) Inhibition of subtilisin BPN' by reaction site P1 mutants of *Streptomyces* subtilisin inhibitor. *J. Biochem.* **109**, 377–382.

Komiyama, T., Bigler, T.L., Yoshida, N., Noda, K. & Laskowski, M., Jr. (1991) Replacement of P1 Leu18 by Glu18 in the reactive site of turkey ovomucoid third domain converts it into a strong inhibitor of Glu-specific *Streptomyces*

griseus proteinase (GluSGP). *J. Biol. Chem.* **266**, 10727–10730.

Komiyama, T., Ray, C.A., Pickup, D.J., Howard, A.D., Thornberry, N.A., Peterson, E.P. & Salvesen, G. (1994) Inhibition of interleukin-1β converting enzyme by the cowpox virus serpin CrmA. *J. Biol. Chem.* **269**, 19331–19337.

Krezel, A.M., Darba, P., Robertson, A.D., Fejzo, J., Macura, S. & Markley, J.L. (1994) Solution structure of turkey ovomucoid third domain as determined from nuclear magnetic resonance data. *J. Mol. Biol.* **242**, 203–214.

Krokoszynska, I. & Otlewski, J. (1996) Thermodynamic stability effects of single peptide bond hydrolysis in protein inhibitors of serine proteinases. *J. Mol. Biol.* **256**, 793–802.

Krokoszynska, I., Dadlez, M. & Otlewski, J. (1998) Structure of single-disulfide variants of bovine pancreatic trypsin inhibitor (BPTI) as probed by their binding to bovine β-trypsin. *J. Mol. Biol.* **275**, 503–513.

Krowarsch, D., Dadlez, M., Buczek, O., Krokoszynska, I., Smalas, A.O. & Otlewski, J. (1999) Interscaffolding additivity: Binding of P_1 variants of bovine pancreatic trypsin inhibitor to four serine proteases. *J. Mol. Biol.* **289**, 175–186.

Krystek, S., Stouch, T. & Novotny, J. (1993) Affinity and specificity of serine endopeptidase–protein inhibitor interactions. *J. Mol. Biol.* **234**, 661–679.

Lapatto, R., Krengel, U., Schreuder, H.A., Arkema, A., de Boer, B., Kalk, K.H., Hol, W.G.J., Grootenhuis, P.D.J., Mulders, J.W.M., Dijkema, R., Theunissen, H.J.M. & Dijkstra, B.W. (1997) X-ray structure of anistasin at 1.9 Å resolution and its modelled complex with blood coagulation factor Xa. *EMBO J.* **16**, 5151–5161.

Laskowski, M., Jr. & Sealock, W.R. (1971) Protein proteinase inhibitors-molecular aspects. *Enzymes* **3**, 376–457.

Laskowski, M., Jr. & Kato, I. (1980) Protein inhibitors of proteinases. *Annu. Rev. Biochem.* **49**, 593–626.

Laskowski, M., Jr. (1986) Protein inhibitors of serine proteinases – mechanism and classification. *Adv. Exp. Med. Biol.* **199**, 1–17.

Laskowski, M., Jr., Kato, I., Ardelt, W., Cook, J., Denton, A., Empie, M.W., Kohr, W.J., Park, S.J., Parks, K., Schatzley, B.L., Tyashiro, M., Vichot, G., Wheatley, H.E., Wieczorek, A. & Wieczorek, M. (1987) Ovomucoid third domains from 100 avian species: Isolation, sequences, and hypervariability of enzyme-inhibitor contact residues. *Biochemistry* **26**, 202– 221.

Lawrence, D.A. (1997) The role of reactive-center loop mobility in the serpin inhibitory mechanism. *Adv. Exp. Med. Biol.* **425**, 99–108.

Lee, G.F., Lazarus, R.A. & Kelley, R.F. (1997) Potent bifunctional anticoagulants: Kunitz domain-tissue factor fusion proteins. *Biochemistry* **36**, 5609–5611.

Lee, K.N., Im, H., Kang, S.W. & Yu, M.-H. (1998) Characterization of a human α_1-antitrypsin variant that is as stable as ovalbumin. *J. Biol. Chem.* **273**, 2509–2516.

Li, J., Wang, Z., Canagarajah, B., Jiang, H., Kanost, M. & Goldsmith, E.J. (1999) The structure of active serpin 1K from *Manduca sexta*. *Structure* **7**, 103–109.

Li de la Sierra, I., Quillien, L., Flecker, P., Gueguen, J. & Brunie, S. (1999) Dimeric crystal structure of a Bowman-Birk protease inhibitor from pea seeds. *J. Mol. Biol.* **285**, 1195–1207.

Liepinsh, E., Berndt, K.D., Sillard, R., Mutt, V. & Otting, G. (1994) Solution structure and dynamics of PEC-60, a protein of the Kazal type inhibitor family, determined by nuclear magnetic resonance spectroscopy. *J. Mol. Biol.* **239**, 137–153.

Lim-Wilby, M.S.L., Hallenga, K., de Maeyer, M., Lasters, I., Vlasuk, G.P. & Brunck, T.K. (1995) NMR structure determination of tick anticoagulant peptide (TAP). *Protein Sci.* **4**, 1178–1186.

Lin, G., Bode, W., Huber, R., Chi, C. & Engh, R.A. (1993) The 0.25 nm X-ray structure of the Bowman-Birk type inhibitor from mung bean in ternary complex with porcine trypsin. *Eur. J. Biochem.* **212**, 549–555.

Liu, J., Praskash, O., Huang, Y., Wen, L., Wen, J.J., Huang, J.-K. & Krishnamoorthi, R. (1996a) Internal mobility of reactive-site-hydrolyzed recombinant *Cucurbita maxima* trypsin inhibitor-V characterized by NMR spectroscopy: Evidence for differential stabilization of newly formed C- and N-termini. *Biochemistry* **35**, 12503–12510.

Liu, J., Prakash, O., Cai, M., Gong, Y., Huang, Y., Wen, L., Wen, J.J., Huang, J.-K. & Krishnamoorthi, R. (1996b) Solution structure and backbone dynamics of recombinant *Cucurbita maxima* trypsin inhibitor-V determined by NMR spectroscopy. *Biochemistry* **35**, 1516–1524.

Lomas, D.A., Elliott, P.R., Chang, W.S.W., Wardell, M.R. & Carrell, R.W. (1995) Preparation and characterization of latent α1-antitrypsin. *J. Biol. Chem.* **270**, 5282–5288.

Löbermann, H., Tokuoka, R., Deisenhofer, J. & Huber, R. (1984) Human α_1-proteinase inhibitor: Crystal structure analysis of two crystal modifications, molecular model and preliminary analysis of the implications for function. *J. Mol. Biol.* **177**, 531–557.

Lu, W., Zhang, W., Molloy, S.S., Thomas, G., Ryan, K., Chiang, Y., Anderson, S. & Laskowski, M., Jr. (1993) Arg^{15}-Lys^{17}-Arg^{18} turkey ovomucoid third domain inhibits human furin. *J. Biol. Chem.* **268**, 14583–14585.

Lu, W., Qasim, M.A., Laskowski, M., Jr. & Kent, S.B.H. (1997a) Probing intermolecular main chain hydrogen bonding in serine proteinase–protein inhibitor complexes: Chemical synthesis of back-engineered turkey ovomucoid third domain. *Biochemistry* **36**, 673–679.

Lu, W., Apostol, I., Qasim, M.A., Warne, N., Wynn, R., Zhang, W.L., Anderson, S., Chiang, Y.W., Ogin, E., Rothberg, I., Ryan, K. & Laskowski, M., Jr. (1997b) Binding of amino acid side chain to S1 cavities of serine proteinases. *J. Mol. Biol.* **266**, 441–461.

Ludvigsen, S., Shen, H., Kjaer, M., Madsen, J.C. & Poulsen, F.M. (1991) Refinement of the three-dimensional solution structure of barley serine proteinase inhibitor 2 and comparison with the structures in crystals. *J. Mol. Biol.* **222**, 621–635.

Lukacs, C.M., Rubin, H. & Christianson, D.W. (1998) Engineering an anion-binding cavity in antichymotrypsin modulates the "spring-loaded" serpin–protease interaction. *Biochemistry* **37**, 3297–3304.

Makhatadze, G.I., Kim, K.S., Woodward, C. & Privalov, P.L. (1993) Thermodynamics of BPTI folding. *Protein Sci.* **2**, 2028–2036.

Markland, W., Ley, A.C. & Ladner, R.C. (1996) Iterative optimization of high affinity protease inhibitors using phage display. 1. Plasmin. *Biochemistry* **35**, 8058–8067.

Mathialagan, N. & Hansen, T.R. (1996) Pepsin-inhibitory activity of the uterine serpins. *Proc. Natl. Acad. Sci. U.S.A.* **93**, 13653–13658.

McGrath, M.E., Engel, T., Bystroff, C. & Fletterick, R.J. (1994) Macromolecular chelation as an improved mechanism: Structure of the ecotin-trypsin complex. *EMBO J.* **13**, 1502–1507.

McGrath, M.E., Gillmor, S.A. & Fletterick, R.J. (1995) Ecotin: Lesson on survival in a protease-filled world. *Protein Sci.* **4**, 141–148.

McPhalen, C.A. & James, M.N.G. (1987) Crystal and molecular structure of the serine proteinase inhibitor CI-2 from barley seeds. *Biochemistry* **26**, 261–269.

McPhalen, C.A. & James, M.N.G. (1988) Structural comparison of two serine proteinase–protein inhibitor complexes: Eglin-c–subtilisin Carlsberg and CI-2–subtilisin Novo. *Biochemistry* **27**, 6582–6598.

Mer, G., Kellenberger, C., Koehl, P., Stote, R., Sorokine, O., Van Dorsselaer, A.M., Luu, B., Hietter, H. & Lefvére, J.-F. (1994) Solution structure of PMP-D2, a 35-residue peptide isolated from the insect *Locusta migratoria*. *Biochemistry* **33**, 15397–15407.

Mer, G., Hietter, H., Kellenberger, C., Renatus, M., Luu, B. & Lefvre, J.-F. (1996) Solution structure of PMP-C: A new fold in the group of small serine proteinase inhibitors. *J. Mol. Biol.* **258**, 158–171.

Merigeau, K., Arnoux, B., Perahia, D., Norris, K. & Ducruix, A. (1998) 1.2 Å of the Kunitz-type domain from the 3 chain of human type VI collagen. *Acta Cryst.* **D54**, 306–312.

Mitsui, Y., Satow, Y. & Sakamaki, T. (1977) Crystal structure of a protein protease inhibitor (*Streptomyces* subtilisin inhibitor) at 2.3 Å resolution. *J. Biochem (Tokyo)* **82**, 295–298.

Mittl, P.R.E., Di Marco, S., Fendrich, G., Pohlig, G., Heim, J., Sommerhoff, C., Fritz, H., Priestle, J.P. & Grütter, M.G. (1996) A new structural class of serine protease inhibitors revealed by the structure of the hirustasin-kallikrein complex. *Structure* **5**, 253–264.

Morenweiser, R., Auerswald, E.A., van de Locht, A., Fritz, H., Strzebecher, J. & Stubbs, M.T. (1997) Structure-based design of a potent chimeric thrombin inhibitor. *J. Biol. Chem.* **272**, 19938–19942.

Moses, E. & Hinz, H.-J. (1983) Basic pancreatic trypsin inhibitor has unusual thermodynamic stability parameters. *J. Mol. Biol.* **170**, 765–776.

Mottonen, J., Strand, A., Symersky, J., Sweet, R.M., Danley, D.E., Geoghegan, K.F., Gerard, R.D. & Goldsmith, E.J. (1992) Structural basis of latency in plasminogen activator inhibitor-1. *Nature* **355**, 270–273.

Mourey, L., Samama, J.-P., Delarue, M., Petitou, M., Choay, J. & Moras, D. (1993) Crystal structure of cleaved bovine antithrombin III at 3.2 Å resolution. *J. Mol. Biol.* **232**, 223–241.

Mühlhahn, P., Czisch, M., Morenweiser, R., Habermann, B., Engh, R.A., Sommerhoff, C.P., Auerswald, E.A. & Holak, T.A. (1994) Structure of leech derived tryptase inhibitor (LDTI-C) in solution. *FEBS Lett.* **355**, 290–296.

Musil, D., Bode, W., Huber, R., Laskowski, M., Jr., Lin, T.-Y. & Ardelt, W. (1991) Refined X-ray crystal structures of the reactive site modified ovomucoid inhibitor third domains from silver pheasant (OMSVP3*) and from Japanese quail (OMJPQ3*). *J. Mol. Biol.* **220**, 739–755.

Nielsen, K.J., Alewood, D., Andrews, J., Kent, S.B.H. & Craik, D.J. (1994a) An 1H NMR determination of the three dimensional structures of mirror image forms of a Leu-5 variant of the trypsin inhibitor from *Ecbalium elaterium* (EETI II). *Protein Sci.* **3**, 291–302.

Nielsen, K.J., Heath, R.L., Anderson, M.A. & Craik, D.J. (1994b) The three dimensional solution structure by ^{1}H NMR of a 6-kDa proteinase inhibitor isolated from the stigma of *Nicotiana alata*. *J. Mol. Biol.* **242**, 231–243.

Nielsen, K.J., Heath, R.L., Anderson, M.A. & Craik, D.J. (1995) Structures of a series of 6-kDa trypsin inhibitors isolated from the stigma of *Nicotiana alata*. *Biochemistry* **34**, 14304–14311.

Neurath, H. (1984) Evolution of proteolytic enzymes. *Science* **224**, 350–357.

Onesti, S., Brick, P. & Blow, D.M. (1991) Crystal structure of a Kunitz-type trypsin inhibitor from *Erythrina caffra* seeds. *J. Mol. Biol.* **217**, 153–176.

Osmark, P., Sorensen, P. & Poulsen, F.M. (1993) Context dependent of protein secondary structure formation: The three-dimensional structure and stability of a hybrid between chymotrypsin inhibitor 2 and helix E from subtilisin Carlsberg. *Biochemistry* **32**, 11007–11014.

Otlewski, J. & Zbyryt, T. (1994) Single peptide bond hydrolysis/resynthesis in squash inhibitors of serine proteinases. I. Kinetics and thermodynamics of the interaction between squash inhibitors and bovine β-trypsin. *Biochemistry* **33**, 200–207.

Otlewski, J., Zbyryt, T., Dryjanski, M., Bulaj, G. & Wilusz, T. (1994) Single peptide bond hydrolysis/resynthesis in squash inhibitors of serine proteinases. II. Limited proteolysis of *Cucurbita maxima* trypsin inhibitor I (CMTI I) by pepsin. *Biochemistry* **33**, 208–213.

Pal, G.P., Kavounis, C.A., Jany, K.D. & Tsernoglou, D. (1994) The three-dimensional structure of the complex of proteinase K with its naturally occurring inhibitor. *FEBS Lett.* **341**, 167–170.

Peng, J.W. & Wagner, G. (1992) Mapping of the spectral densities of N–H bond motions in eglin c using heteronuclear relaxation experiments. *Biochemistry* **31**, 8571–8586.

Pereira, P.J., Bergner, A., Macedo-Riberio, S., Huber, R., Matschiaer, G., Fritz, H., Sommerhoff, C.P. & Bode, W. (1998) Human

beta-tryptase is aring-like treatment with active sites facing a central pore. *Nature* **392**, 306–311.

Perona, J.J., Tsu, C.A., Fletterick, R.J. & Craik, C.S. (1993) Crystal structures of rat anionic trypsin complexed with the protein inhibitors APPI and BPTI. *J. Mol. Biol.* **230**, 919–933.

Perona, J.J., Tsu, C.A., Craik, C.S. & Fletterick, R.J. (1997) Crystal structure of an ecotin- collagenase complex suggests a model for recognition and cleavage of the collagen triple helix. *Biochemistry* **36**, 5381–5392.

Polanowska, J., Krokoszynska, I., Czapinska, H., Watorek, W., Dadlez, M. & Otlewski, J. (1998) Specificity of human cathepsin G. *Biochim. Biophys. Acta* **1386**, 189–198.

Potempa, J., Korzus, E. & Travis, J. (1994) The serpin superfamily of proteinase inhibitors: structure, function, and regulation. *J. Biol. Chem.* **269**, 15957–15960.

Priestle, J.P. & Di Marco, S. (1997) Structure of the complex of leech-derived tryptase inhibitor (LDTI) with trypsin and modeling of the LDTI–tryptase system. *Structure* **5**, 1465–1474.

Qasim, M.A., Ranjbar, M.R., Wynn, R., Anderson, S. & Laskowski, M., Jr. (1995) Ionizable P1 residues in serine proteinase inhibitors undergo large pK shifts on complex formation. *J. Biol. Chem.* **270**, 1–4.

Qasim, M.A., Ganz, P.J., Saunders, C.W., Bateman, K.S., James, M.N.G. & Laskowski, M., Jr. (1997) Interscaffolding additivity. Association of P_1 variants of eglin c and of turkey ovomucoid third domain with serine proteinases. *Biochemistry* **36**, 1598–1607.

Quast, U., Engel, J., Steffen, E., Tschesche, H. & Kupfer, S. (1978) Kinetics of the interaction of α-chymotrypsin with trypsin kallikrein inhibitor (Kunitz) in which the reactive-site peptide bond Lys-15-Ala16 is split. *Eur. J. Biochem.* **86**, 353–360.

Read, R.J., Fujinaga, M., Sielecki, A.R. & James, M.N.G. (1983) Structure of the complex of *Streptomyces griseus* protease B and the third domain of the turkey ovomucoid inhibitor at 1.8 Å resolution. *Biochemistry* **22**, 4420–4433.

Roberts, B.L., Markland, W., Ley, A.C., Kent, R.B., White, D.W., Guterman, S.K. & Ladner, R.C. (1992) Directed evolution of a protein: Selection of potent neutrophil elastase inhibitors displayed on M13 fusion phages. *Proc. Natl. Acad. Sci. U.S.A.* **89**, 2429–2433.

Rydel, T.J., Ravichandran, K.G., Tulinsky, A., Bode, W., Huber, R., Roitsch, C. & Fenton, J.W. (1990) The structure of a complex of recombinant hirudin and human α-thrombin, *Science* **249**, 277–280.

Rydel, T.J., Tulinsky, A., Bode, W. & Huber, R. (1991) Refined structure of the hirudin–thrombin complex. *J. Mol. Biol.* **221**, 583–601.

Ryu, S.-E., Choi, H.-J., Kwon, K.-S., Lee, K.N. & Yu, M.-H. (1996) The native strains in the hydrophobic core and flexible reactive loop of a serine protease inhibitor: Crystal structure of an uncleaved α_1-antitrypsin at 2.7 Å. *Structure* **4**, 1181–1192.

Schechter, I. & Berger, A. (1967) On the size of the active site in proteases. *Biochem. Biophys. Res. Commun.* **27**, 157–162.

Scheidig, A.J., Hynes, T.R., Pelletier, L.A., Wells, J.A. & Kossiakoff, A.A. (1997) Crystal structures of bovine chymotrypsin and trypsin complexed to the inhibitor domain of Alzheimer's amyloid β-precursor (APPI) and basic pancreatic trypsin inhibitor (BPTI): Engineering of inhibitors with altered specificities. *Protein Sci.* **6**, 1806–1824.

Schreuder, H.A., de Boer, B., Dijkema, R., Mulders, J., Theunissen, H.J.M., Grootenhuis, P.D.J. & Hol, W.G.J. (1994) The intact and cleaved human antithrombin III complex as a model for serpin-proteinase interactions. *Nature Struct. Biol.* **1**, 48–54.

Schulze, A.J., Baumann, U., Knof, S., Jaeger, E., Huber, R. & Laurell, C.B. (1990) Structural transition of alpha 1-antitrypsin by a peptide sequentially similar to beta-strand s4A. *Eur. J. Biochem.* **194**, 51–56.

Seeram, S.S., Hiraga, K. & Oda, K. (1997) Peptide bond and temporary inhibition of *Streptomyces* metalloproteinase inhibitor. *J. Biochem. (Tokyo)* **122**, 788–794.

Sharp, A.M., Stein, P.E., Pannu, N.S., Carrell, R.W., Berkenpas, M.B., Ginsburg, D., Lawrence, D.A. & Read, R.J. (1999) The active conformation of plasminogen activator inhibitor 1, a target for drugs to control fibrinolysis and cell adhesion. *Structure* **7**, 111–118.

Shaw, G.L., Davis, B., Keeler, J. & Fersht, A.R. (1995) Backbone dynamics of chymotrypsin inhibitor 2: Effect of breaking the active site bond and its implications for the mechanism of inhibition of serine proteases. *Biochemistry* **34**, 2225–2233.

Shin, D.H., Song, H.K., Seong, I.S., Lee, C.S., Chung, C.H. & Suh, S.W. (1996) Crystal structure analyses of uncomplexed ecotin in two crystal forms: Implications for its function and stability. *Protein Sci.* **5**, 2236–2247.

Shore, J.D., Day, D.E., Francis-Chmura, A.M., Verhamme, I., Kvasman, J., Lawrence, D.A. & Ginsburg, D. (1995) A fluorescent probe of plasminogen activator inhibitor-1. Evidence for reactive center loop insertion and its role in the inhibitory mechanism. *J. Biol. Chem.* **270**, 5395–5398.

Siekmann, J., Wenzel, H.R., Matuszak, E., von Goldammer, E. & Tschesche, H. (1988) The pH dependence of the equilibrium constant K_{hyd} for the hydrolysis of the Lys^{15}-Ala^{16} reactive-site peptide bond in bovine pancreatic trypsin inhibitor (aprotinin). *J. Prot. Chem.* **7**, 633–640.

Skinner, R., Abrahams, J.-P., Whisstock, J.C., Lesk, A.M., Carrell, R.W. & Wardell, M.R. (1997) The 2.6 Å structure of antithrombin indicates a conformational change at the heparin binding site. *J. Mol. Biol.* **266**, 601–609.

Skinner, R., Chang, W.S.W., Jin, L., Pei, X., Huntington, J.A., Abrahams, J.P., Carrell, R.W. & Lomas, D.A. (1998) Implications for function and therapy of a 2.9 Å structure of binary-complexed antithrombin. *J. Mol. Biol.* **283**, 9–14.

Song, H.K. & Suh, S.W. (1998) Kunitz-type soybean trypsin inhibitor revisited: Refined structure of its complex with porcine trypsin reveals an insight into the interaction between a homologous inhibitor from *Erythrina caffra* and tissue-type plasminogen activator. *J. Mol. Biol.* **275**, 347–363.

Stein, P.E., Tewkesbury, C. & Carrell, R.W. (1989) Ovalbumin and angiotensinogen lack serpin S-R conformational change. *Biochem. J.* **262**, 103–107.

Stein, P., Leslie, A.G.W., Finch, J.T., Turnell, W.G., McLaughlin, P.J. & Carrell, R.W. (1990) Crystal structure of ovalbumin as a model for the reactive center of serpins. *Nature* **347**, 99–102.

Stein, P., Leslie, A.G.W., Finch, J.T. & Carrell, R.W. (1991) Crystal structure of uncleaved ovalbumin at 1.95 Å resolution. *J. Mol. Biol.* **221**, 941–959.

Stein, P.E. & Carrell, R.W. (1995) What do dysfunctional serpins tell us about molecular mobility and disease? *Nature Struct. Biol.* **2**, 96–113.

Stone, S.R., Whisstock, J.C., Bottomely, S.P. & Hopkins, P.C.R. (1997) Serpins. A mechanistic class of their own. *Adv. Exp. Med. Biol.* **425**, 5–15.

Strobl, S., Mühlhahn, P., Bernstein, R., Wiltscheck, R., Maskos, K., Wunderlich, M., Huber, R., Glockshuber, R. & Holak, T.A. (1995) Determination of the three-dimensional structure of the bifunctional α-amylase/trypsin inhibitor from ragi seeds by NMR spectroscopy. *Biochemistry* **34**, 8281–8293.

Strobl, S., Maskos, K., Wiegand, G., Huber, R., Gomis-Rüth, F.X. & Glockshuber, R. (1998) A novel strategy for inhibition of α-amylases: Yellow meal worm α-amylase in complex with the ragi bifunctional inhibitor at 2.5 Å resolution. *Structure* **6**, 911–921.

Stubbs, M.T. & Bode, W. (1995) The clot thickens: Clues provided by thrombin structure. *Trends Biochem. Sci.* **20**, 23–28.

Stubbs, M.T., Morenweiser, R., Stürzebecher, J., Bauer, M., Bode, W., Huber, R., Piechottka, G.P., Matschiner, G., Sommerhoff, C.P., Fritz, H. & Auerswald, E.A. (1997) The three-dimensional structure of recombinant leech-derived tryptase inhibitor in complex with trypsin. *J. Biol. Chem.* **272**, 19931–19937.

Suzuki, A., Yamane, T., Ashida, T., Norioka, S., Hara, S. & Ikenaka, T. (1993) Crystallographic refinement of Bowman-Birk type proteases inhibitor A-II from peanut (*Arachis hypogaea*) at 2.3 Å resolution. *J. Mol. Biol.* **234**, 722–734.

Szyperski, T., Güntert, P., Stone, S.R. & Wüthrich, K. (1992a) Nuclear magnetic resonance solution structure of hirudin(1-51) and comparison with corresponding three-dimensional structures determined using the complete 65-residue hirudin polypeptide chain. *J. Mol. Biol.* **228**, 1193–1205.

Szyperski, T., Güntert, P., Stone, S.R., Tulinsky, A., Bode, W., Huber, R. & Wüthrich, K. (1992b) Impact of protein–protein contacts on the conformation of thrombin-bound hirudin studied by comparison with the nuclear magnetic resonance solution structure of hirudin (1-51). *J. Mol. Biol.* **228**, 1206–1211.

Takeuchi, Y., Satow, Y., Nakamura, K.T. & Mitsui, Y. (1991) Refined crystal structure of the complex of subtilisin BPN′ and *Streptomyces* subtilisin inhibitor at 1.8 Å resolution. *J. Mol. Biol.* **221**, 309–325.

Takeuchi, Y., Nonaka, T., Nakamura, K.T., Kojima, S., Miura, K.-I. & Mitsui, Y. (1992) Crystal structure of an engineered subtilisin inhibitor complexed with bovine trypsin. *Proc. Natl. Acad. Sci. U.S.A.* **89**, 4407–4411.

Tamura, A., Kanaori, K., Kojima, S., Kumagai, I., Miura, K. & Akasaka, K. (1991) Mechanism of temporary inhibition in *Streptomyces* subtilisin inhibitor induced by an amino acid substitution, tryptophan 86 replaced by histidine. *Biochemistry* **30**, 5275–5286.

Travis, J. & Salvesen, G.S. (1983) Human plasma proteinase inhibitors. *Annu. Rev. Biochem.* **52**, 655–709.

Tsunemi, M., Matsuura, Y., Sakakibara, S. & Katsube, Y. (1996) Crystal structure of an elastase-specific inhibitor elafin complexed with porcine pancreatic elastase determined at 1.9 Å resolution. *Biochemistry* **35**, 11570–11576.

Tsunogae, Y., Tanaka, I., Yamane, T., Kikkawa, J., Achida, J.T., Ishikawa, C., Watanabe, K., Nakamura, S. & Takahashi, K. (1986) Structure of the trypsin-binding domain of Bowman-Birk type protease inhibitor and its interaction with trypsin. *J. Biochem (Tokyo)* **100**, 1637–1646.

Tucker, H.M., Mottonen, J., Goldsmith, E.J. & Gerard, R.D. (1995) Engineering of plasminogen activator inhibitor-1 to reduce the rate of latency transition. *Nature Struct. Biol.* **2**, 442–445.

Uson, I., Sheldrick, G.M., de La Fortelle, E., Bricogne, G., Di Marco, S., Priestle, J.P. & Grutter, M.G. (1999) The 1.2 Å crystal structure of hirustasin reveals the intrinsic flexibility of a family of highly disulphide-bridged serine proteases. *Structure* **7**, 55–63.

Vallee, F., Kadziola, A., Bourne, Y., Juy, M., Rodenburg, K.W., Svensson, B. & Haser, R. (1998) Barley α-amylase bound to its endogenous protein inhibitor BASI: Crystal structure of the complex at 1.9 Å resolution. *Structure* **6**, 649–659.

van de Locht, A., Lamba, D., Bauer, M., Huber, R., Friedrich, T., Kroger, B., Hoffken, W. & Bode, W. (1995) Two heads are better than one: Crystal structure of the insect derived double domain Kazal inhibitor rhodniin in complex with thrombin. *EMBO J.* **14**, 5149–5157.

van de Locht, A., Stubbs, M.T., Bode, W., Friedrich, T., Bollschweiler, C., Hoffken, W. & Huber, R. (1996) The ornithodorin-thrombin crystal structure, a key to the TAP enigma? *EMBO J.* **22**, 6011–6017.

van de Locht, A., Bode, W., Huber, R., Le Bonniec, B.F., Stone, S.R., Esmon, C.T. & Stubbs, M.T. (1997) The thrombin E192Q-BPTI complex reveals gross structural rearrangements for the interaction with antithrombin and thrombomodulin. *EMBO J.* **16**, 2977–2984.

Walkenhorst, W.F., Krezel, A.M., Rhyu, G.I. & Markley, J.L. (1994) Solution structure of reactive site hydrolyzed turkey ovomucoid third domain by nuclear magnetic resonance and distance geometry methods. *J. Mol. Biol.* **242**, 215–230.

Wardell, M.R., Abrahams, J.P., Bruce, D., Skinner, R. & Leslie, A.G. (1993) Crystallization and preliminary X-ray diffraction analysis of

two conformations of intact human antithrombin. *J. Mol. Biol.* **234**, 1253–1258.

Waxman, L., Smith, D.E., Arcuri, K.E. & Vlasuk, G.P. (1990) Tick anticoagulant peptide (tap) is a novel inhibitor of blood coagulation factor Xa. *Science* **248**, 593–596.

Wei, A., Rubin, H., Cooperman, B.S. & Christianson, D.W. (1994) Crystal structure of an uncleaved serpin reveals the conformation of an inhibitory reactive loop. *Nature Struct. Biol.* **1**, 251–257.

Wei, A., Alexander, R.S., Duke, J., Ross, H., Rosenfeld, S.A. & Chang, C.H. (1998) Unexpected binding mode of tick anticoagulant peptide complexed to bovine factor Xa. *J. Mol. Biol.* **283**, 147–154.

Wells, J.A. (1990) Additivity of mutational effects in proteins. *Biochemistry* **29**, 8509–8517.

Werner, M.H. & Wemmer, D.E. (1992) Three-dimensional structure of soybean trypsin/chymotrypsin Bowman-Birk inhibitor in solution. *Biochemistry* **31**, 999–1010.

Whisstock, J., Skinner, R. & Lesk, A.M. (1998) An atlas of serpin conformations. *Trends Biochem. Sci.* **23**, 63–67.

Wlodawer, A., Walter, J., Huber, R. & Sjolin, L. (1984) Structure of bovine pancreatic trypsin inhibitor. Results of joint neutron and X-ray refinement of crystal form II. *J. Mol. Biol.* **180**, 301–329.

Wright, H.T. & Scarsdale, J.N. (1995) Structural basis for serpin inhibitor activity. *Proteins: Struct. Funct. Genet.* **22**, 210–225.

Wright, H.T., Qian, H.Z. & Huber, R. (1990) Crystal structure of plakalbumin, a proteolytically nicked form of ovalbumin. *J. Mol. Biol.* **213**, 513–528.

Xu, Y., Carr, P.D., Guss, J.M. & Ollis, D.L. (1998) The crystal structure of bikunin from the inter α-inhibitor complex: A serine protease inhibitor with two Kunitz domains. *J. Mol. Biol.* **276**, 955–966.

Yang, S.Q., Wang, C.-I., Gillmor, S.A., Fletterick, R.J. & Craik, C.S. (1998) Ecotin: A serine protease inhibitor with two distinct and interacting binding sites. *J. Mol. Biol.* **279**, 945–957.

Yu, M.-H., Weissman, J.S. & Kim, P.S. (1995) Contribution of individual side-chains to the stability of BPTI examined by alanine-scanning mutagenesis. *J. Mol. Biol.* **249**, 388–397.

Zbyryt, T. & Otlewski, J. (1991) Interaction between squash inhibitors and bovine trypsinogen. *Biol. Chem. Hoppe-Seyler* **372**, 255–262.

Zemke, K.J., Müller-Farhnow, A., Jany, K.-D., Pal, G.P. & Saenger, W. (1991) The three-dimensional structure of the bifunctional proteinase K/α-amylase inhibitor from wheat (PKI3) at 2.5 Å resolution. *FEBS Lett.* **279**, 240–242.

Zhang, E., St. Charles, R. & Tulinsky, A. (1999) Structure of extracellular tissue factor complexed with factor VII_a inhibited with a BPTI mutant. *J. Mol. Biol.* **285**, 2089–2104.

Zweckstetter, M., Czisch, M., Mayer, U., Chu, M.-L., Zinth, W., Timpl, R. & Holak, T.A. (1995) Structure and multiple conformations of the Kunitz-type domain from human type VI collagen α3(VI) chain in solution. *Structure* **4**, 195–209.